A Journey toward the High-Pressure Metamorphism in Continental Crust: P-T-D Path Estimate and 40Ar/39Ar Single Grain Dating on Muscovite of a Tectonic Unit along the Western Edge of the Alpine Corsica (France)

Maria Di Rosa[1], Edoardo Sanità[2], Chiara Frassi[3], Jean-Marc Lardeaux[4], Michel Corsini[5], Michele Marroni[6], and luca pandolfi[7]

[1]Pisa University
[2]Dipartimento di Scienze della Terra, Università di Firenze
[3]Dipartimento di Scienze della Terra, Università di Pisa
[4]Université Cote d'Azur
[5]Université Côte d'Azur, IRD, CNRS
[6]dipartimento di scienze della Terra, Università di Pisa
[7]Università di Pisa

November 24, 2022

Abstract

The first attempt of pressure-temperature-deformation-time (P-T-d-t) path reconstruction for the Lower Units (Alpine Corsica, France) is presented in this work. The Lower Units represent, together with the Tenda Massif, fragments of the European continental margin involved into the east-dipping Alpine subduction. The new data of thermobarometry applied on metapelites and the new $^{40}Ar/^{39}Ar$ dating of syn-kinematic muscovite sampled into a metagranitoids allowed to define the P-T conditions and the age of the metamorphism of Venaco Unit, a Lower Unit located in the southernmost sector of the Alpine Corsica. The outcoming scenario indicates that the Venaco Unit reached the baric peak at [?] 33 km of depth not before the Bartonian time. At 35.7 Ma (i.e., during the middle Priabonian), it was exhumed at shallower structural level (i.e., at [?] 26 km of depth) mainly through the activation the top-to-the W shear zones. This retrograde path suggests that Venaco Unit experienced a fast exhumation, unlike the Tenda Massif which has already involved into subduction during the Ypresian and stationed at 25-30 km before its exhumation in the Priabonian.

Hosted file

`mdr solidearth_suppinfo.docx` available at https://authorea.com/users/548827/articles/603261-a-journey-toward-the-high-pressure-metamorphism-in-continental-crust-p-t-d-path-estimate-and-40ar-39ar-single-grain-dating-on-muscovite-of-a-tectonic-unit-along-the-western-edge-of-the-alpine-corsica-france

Hosted file

`essoar.10512123.1.docx` available at https://authorea.com/users/548827/articles/603261-a-journey-toward-the-high-pressure-metamorphism-in-continental-crust-p-t-d-path-estimate-and-40ar-39ar-single-grain-dating-on-muscovite-of-a-tectonic-unit-along-the-western-edge-of-the-alpine-corsica-france

M. Di Rosa[1]*, E. Sanità[1,2], C. Frassi[1], J. M. Lardeaux[3,4], M. Corsini[3,4], M. Marroni[1,5] and L. Pandolfi[1]

[1] Università di Pisa, Dipartimento di Scienze della Terra, Via Santa Maria, 53, Pisa, Italia

[2] Università di Firenze, Dipartimento di Scienze della Terra, Via La Pira, 4, Firenze, Italia

[3] Université Côte d'Azur, IRD, CNRS, Observatoire de la Côte d'Azur, Géoazur, 250 rue Albert Einstein, Sophia Antipolis 06560 Valbonne, France

[4] Centre for Lithospheric Reseach, Czech Geological Survey, Kràlov, 3, Prague, Czech Republic

[5] Consiglio Nazionale della Ricerca, Istituto di Geoscienze e Georisorse, IGG-CNR, Via Moruzzi 1, Pisa, Italia

*Corresponding author: Maria Di Rosa (maria.dirosa@unipi.it)

Key Points:

- Tectonic constrains related to the behaviour of the continental-derived units during exhumation processes.
- Definition of the continental-derived Venaco Unit belonging to the Lower Units group of the Alpine Corsica.
- First attempt of reconstruction of the pressure-temperature-deformation-time path of the Venaco Unit.

Abstract

The first attempt of pressure-temperature-deformation-time (P-T-d-t) path reconstruction for the Lower Units (Alpine Corsica, France) is presented in this work. The Lower Units represent, together with the Tenda Massif, fragments of the European continental margin involved into the east-dipping Alpine subduction. The new data of thermobarometry applied on metapelites and the new $^{40}Ar/^{39}Ar$ dating of syn-kinematic muscovite sampled into a metagranitoids allowed to define the P-T conditions and the age of the metamorphism of Venaco Unit, a Lower Unit located in the southernmost sector of the Alpine Corsica. The outcoming scenario indicates that the Venaco Unit reached the baric peak at 33 km of depth not before the Bartonian time. At 35.7 Ma (i.e., during the middle Priabonian), it was exhumed at shallower structural level (i.e., at 26 km of depth) mainly through the activation the top-to-the W shear zones. This retrograde path suggests that Venaco Unit experienced a fast exhumation, unlike the Tenda Massif which has already involved into subduction during the Ypresian and stationed at 25-30 km before its exhumation in the Priabonian.

Plain Language Summary

In this article we propose a tectonic model capable of explaining the behavior of the continental crust involved in the processes of subduction and exhumation.

Our approach to understanding the complexity of a collisional belt consisted in acquiring field and laboratory data and then interpreting them as a whole. The stratigraphic and structural analysis, microtectonics, thermobarometry and geochronology that we present as exclusive data in this work constitute the geological constraints of our geodynamic model, able to explain the different paths that the tectonic units follow after their burial up to the surface.

The study area is located along the boundary between the Hercynian Corsica and the Alpine Corsica (France), where several continental and oceanic tectonic units are stacked. The results of this work points out that the Europe-derived units were buried at different depths ranging from 20 to 35 km at different times from early to late Eocene, and then exhumed following different trajectories and with different exhumation rates.

Keywords

European-derived unit, Lower Units (Alpine Corsica), blueschist facies conditions, Alpine metamorphism, cold vs. warm exhumation path.

1 Introduction

The tectono-metamorphic study of deformed rocks helps to constrain the evolution of collisional belts. Modeling pressure (P) and temperature (T) conditions through time (t) (P-T-t path) of oceanic and continental tectonic units led to individuate the events of the oceanic/continental subduction and the subsequent progressive exhumation that characterize the evolution of worldwide collisional belts. Because of their ability to binding the history of tectonic units in space and time, P-T-t paths have achieved a great success over the past thirty years in the study of metamorphic rocks (e.g., Spear, 1993). One of the most investigated collisional belts is represented by the Alps where the study of rocks recording a wide range of deformation regimes and metamorphic conditions helped to highlight the geodynamic evolution of this belt (e.g., Lardeaux & Spalla, 1991; Handy et al., 2010).

The Alpine Corsica (France) is interpreted as the southern branch of the Western Alps (Mattauer et al., 1981; Durand-Delga, 1984; Marroni & Pandolfi, 2003; Molli & Malavieille, 2011). It consists of a tectonic stack of oceanic and continental units affected by a metamorphism varying from blueschist-eclogite to very low-grade facies conditions acquired in the Late Cretaceous – early Oligocene time span during their involvement into subduction and continental collision originated by the closure of the Ligure-Piemontese oceanic basin (Elter & Pertusati, 1973; Lagabrielle & Polino, 1988; Schmidt et al., 1996; Malavieille et al., 1998; Michard & Martinotti, 2002; Molli, 2008; Handy et al., 2010). Several continental-affinity slices, known as Lower Units, experienced blueschists facies metamorphism (Bezert & Caby, 1988; Malasoma & Marroni, 2007; Molli, 2008; Maggi et al., 2012; Di Rosa et al., 2017a). They were deeply investigated because their tectono-metamorphic evolution provided useful information on the continental subduction stage (i.e., the transition between subduction and collision stages). Even if their P-T paths were obtained by several authors (Molli et

al., 2006; Malasoma & Marroni, 2007; Di Rosa et al., 2019a; Frassi et al., 2022) no data are available to constrain the age of metamorphism.

In this work, we present a multidisciplinary dataset that includes micro- to meso-structural data, thermo-baric estimates, and muscovite $^{40}Ar/^{39}Ar$ single grain dating from one of the southernmost slices belonging to the Lower Units. The result is the first Pressure-Temperature-deformation-time (P-T-d-t) path for the continental units exposed in the western rim of the Alpine Corsica. We discuss these new data to provide new geodynamic implication of the Alpine collisional belt.

2 Geological setting

The Corsica Island includes two geological domains, the Hercynian and Alpine Corsica, exposed in the south-west and north-east areas of the island, respectively (Fig. 1). The Hercynian Corsica consists of a polymetamorphic basement recording Panafrican and Variscan orogenic events intruded by Permo-Carboniferous magmatic rocks (Cabanis et al., 1990; Ménot & Orsini, 1990; Laporte et al., 1991; Rossi et al., 1994; Paquette et al., 2003; Rossi et al., 2009). This basement is covered by sedimentary successions including Permian volcaniclastic and Mesozoic, mainly carbonates, sedimentary rocks unconformably covered by middle to late Eocene siliciclastic turbidites (Durand-Delga, 1984; Rossi et al., 1994; Ferrandini et al., 2010; Di Rosa et al., 2020a). Overall, the Hercynian Corsica is representative of the European continental margin previously regarded as unaffected by Alpine metamorphism and deformation (e.g., Durand-Delga. 1984). The presence of localized shear zones of Tertiary ages affecting the late-Variscan magmatic suite (Di Vincenzo et al., 2016), and Eocene siliciclastic turbidites achieving blueschist metamorphic conditions (Di Rosa et al., 2020a; Di Rosa, 2021), however, suggest that the easternmost rim of Hercynian Corsica was instead involved in the Alpine orogeny.

The Alpine Corsica consists of a stack of continental, transitional and oceanic units strongly deformed and affected by Cretaceous to Tertiary pervasive deformation and metamorphism, ranging from sub-greenschist to blueschist-eclogite facies (e.g., Durand-Delga, 1984; Amaudric du Chaffaut & Saliot, 1979; Mattauer et al., 1981; Dallan & Nardi, 1984; Gibbons & Horak, 1984; Bezert & Caby, 1988; Malavieille et al., 1998; Marroni & Pandolfi, 2003; Malasoma et al., 2006; Levi et al., 2007; Vitale Brovarone et al., 2012). The Alpine Corsica overthrusts the Hercynian domain through NNW-SSE trending, high-angle dipping thrust that runs across the entire island (e.g., Durand-Delga, 1984) (Fig. 1). The architecture of the Alpine Corsica mainly results from the convergence-related processes started since Late Cretaceous that initially produced the closure of an oceanic basin (the Liguro-Piemontese basin) opened between the Europe and Adria margins during Middle to Late Jurassic (Favre & Stampfli, 1992; Manatschal, 1995; Froitzheim & Manatschal, 1996; Bill et al., 1997; Marroni & Pandolfi, 2007). These processes produced an east-dipping subduction of the oceanic lithosphere below the Adria plate leading to development of an Alpine accretionary wedge along the ocean-continent transition at the Adria

plate margin. The progressive subduction of oceanic lithosphere caused the closure of the Liguro-Piemontese basin and the consequent collision between the European continental margin and the Alpine orogenic wedge during the middle Eocene-early Oligocene (Mattauer & Proust, 1976; Gibbons & Horak, 1984; Bezert & Caby, 1988; Malavieille et al., 1998; Malasoma et al., 2006; Molli et al., 2006; Maggi et al., 2012; Di Rosa et al., 2020b). Simultaneously, the portion of the Ligure-Piemontese oceanic lithosphere not yet involved into underthrusting started to subduct toward the west below the European margin. This drastic change in the geodynamic scenario resulted in the large-scale extension of Alpine Corsica thus producing the collapse and thermal re-equilibration of the previously thickened Alpine orogenic wedge and the consequent opening of two back arc basins (the Liguro-Provençal and the Tyrrhenian Sea basins) that separated the Corsica-Sardinia continental microplate from the neighboring domains of the Alpine and Apennine collisional belt, respectively (Jolivet et al., 1991; Fournier et al., 1991; Jolivet et al., 1991, 1998; Daniel et al., 1996; Brunet et al., 2000; Jakni et al., 2000; Zarki-Jakni et al., 2004). Apatite fission track ages obtained by Danišik et al. (2007; 23 Ma) might supports this event of thermal re-equilibration (Di Rosa et al., 2020a).

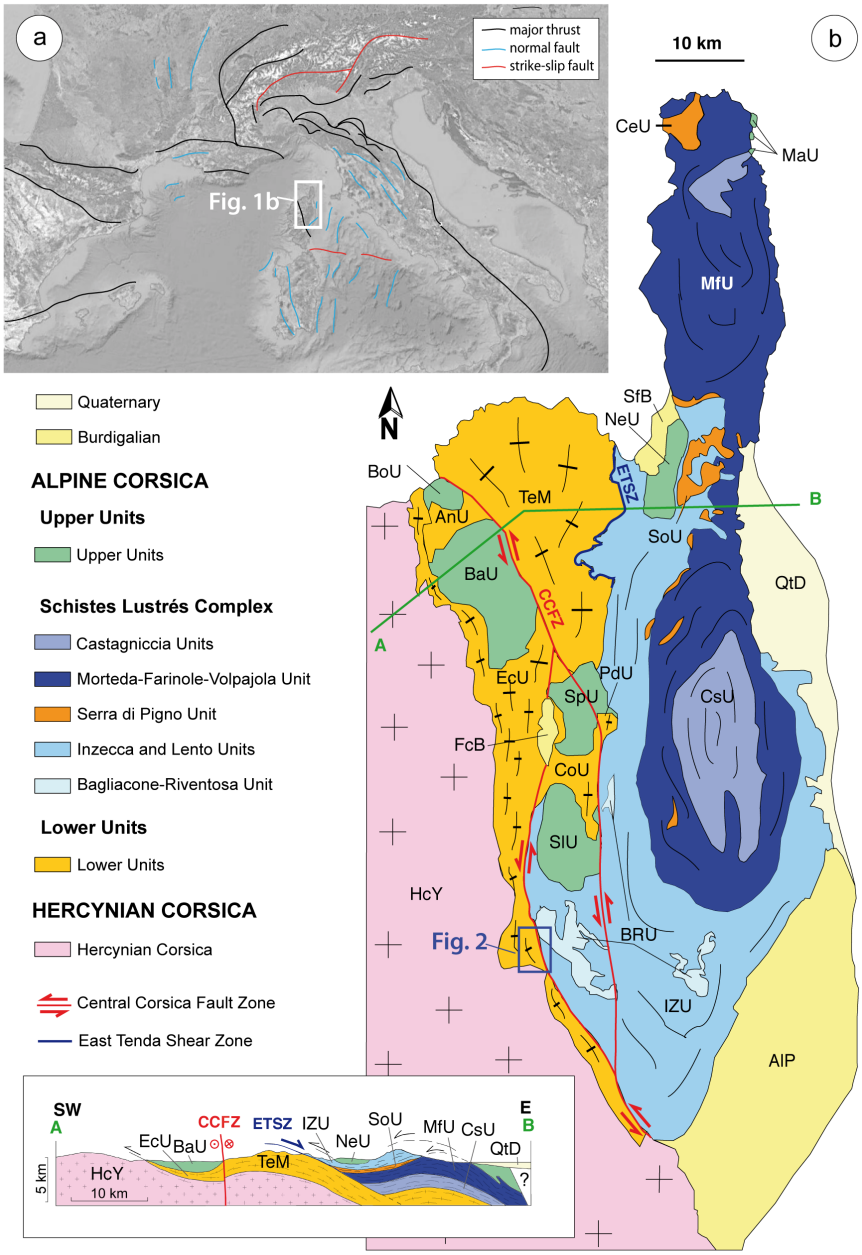

Figure 1. (a) Localization of the study area into the western Mediterranean Sea. (b) Tectonic map of the north-eastern Corsica (modified after Di Rosa et al., 2020b) and schematic cross section (after Di Rosa et al., 2017a). QtD: Quaternary deposits, SfB: Saint-Florent Basin, FcB: Francardo Basin, AlP: Aleria Plain, MaU: Macinaggio

Unit, BoU: Bas-Ostriconi Unit, BaU: Balagne Unit, NeU: Nebbio Unit, SpU: Serra Debbione and Pineto Units, SlU: Santa Lucia Unit, CsU: Castagniccia Unit, MfU: Morteda-Farinole-Volpajola Unit, SoU: Serra di Pigno and Oletta Units, IZU: Inzecca and Lento Units, BrU: Bagliacone- Riventosa Unit, CeU: Centuri Unit, TeM: Tenda Massif, AnU: Annunciata Unit, EcU: External Continental Units, PdU: Cima Pedani Units, CoU: Caporalino Unit, HcY: Hercynian Corsica. The location of the study area is marked by a blue rectangle.

The Alpine Corsica can be subdivided from top to the bottom in: the Upper Units, the Schistes Lustrés Complex and the Lower Units. The Upper Units and the Schistes Lustrés Complex (Fig.1) preserve record of the subduction process. The Upper Units include slices of oceanic lithosphere characterized by very low-grade metamorphism achieved during their involvement in the subduction at higher structural level simultaneously to the Schistes Lustrés Complex (Durand-Delga et al., 1997; Saccani et al., 2000; Marroni & Pandolfi, 2003; Pandolfi et al., 2016). The Schistes Lustrés Complex is composed of oceanic and oceanic-continental units with high pressure-low temperature (HP-LT) metamorphic imprint (e.g., Faure & Malavieille, 1981; Caron & Péquignot, 1986; Warburton, 1986; Waters, 1990; Fournier et al., 1991; Guieu et al., 1994; Levi et al., 2007; Chopin et al., 2008; Ravna et al., 2010; Meresse et al., 2012; Vitale Brovarone et al., 2014) ranging in age between Late Cretaceous (Lahondère & Guerrot, 1997; Maluski, 1977; Brunet et al., 2000) to late Eocene (Brunet et al., 2000; Martin et al., 2011; Vitale Brovarone & Herwartz, 2013). The Lower Units consist of continental crust slices derived from the thinned European margin involved in the subduction and accreted to the orogenic wedge. They show the same stratigraphic log of the Hercynian Corsica but are affected by blueschists facies metamorphism (e.g., Gibbons & Horak, 1984; Brunet et al., 2000; Tribuzio & Giacomini, 2002; Gueydan et al., 2003; Molli et al., 2006; Malasoma & Marroni, 2007; Maggi et al., 2012; Di Rosa et al., 2019b). The Lower Units registered a polyphase deformation history with three ductile events (Bezert & Caby, 1988; Malasoma & Marroni, 2007; Garfagnoli et al., 2009; Di Rosa et al., 2019a) achieved during the beginning of the exhumation (D1 phase), the exhumation within the subduction channel (D2 phase) and the final emplacement at shallower crustal levels in the extensional setting induced by the orogenic collapse (D3 phase). Paleontological data indicate that the deposition of the Alpine foredeep deposits (breccias and sandstones) on the European continental margin occurs in the Lutetian-Priabonian (*Nummulite* sp., Amaudric du Chaffaut et al., 1985; Bezert & Caby, 1988; Ferrandini et al., 2010; Di Rosa et al., 2017a). The age of the HP-LT metamorphism achieved by the European-affinity continental units was constrained only for the Tenda Massif where Brunet et al. (2000) and Maggi et al. (2012) detected early to late Eocene ages. Similar ages were obtained for the shear zones located within the Hercynian Corsica (e.g., Razzo Bianco area) by Di Vincenzo et al. (2016).

After the D3 phase, a sinistral strike-slip fault system (i.e., Central Corsica Shear Zone - CCSZ; Central Corsica Fault Zone – CCFZ of Waters, 1990; Ostriconi

Fault of Lacombe & Jolivet, 2005) (Fig. 1) cut both the stack of the Alpine Corsica and its western boundary with the Hercynian domain. The CCFZ is an important north-south trending regional-scale structure (Maluski et al., 1973; Lacombe & Jolivet, 2005; Di Rosa et al., 2017b; Malasoma et al., 2020; Frassi et al., 2022) stretching from the north, where it bounds the western side of the Tenda Massif, toward to south where it splits in two branches in correspondence of the Asco valley (Fig. 1). Although there is no dating available to constrain the CCFZ activity, it is constrained by the age of the youngest deposits deformed by faults (i.e., the Lutetian-Priabonian foredeep deposits), and by the oldest deposits sealing the CCFZ structures (i.e., the Burdigalian-Langhian deposits of the Francardo basin; Alessandri et al., 1977; Ferrandini et al., 1998; Malasoma et al., 2020).

3 Methods

The techniques used in this work are: (1) structural mapping and mesoscale structural analysis, (2) microtectonic study of selected samples of metagranitoids and Permian metavolcaniclastics, (3) thermobarometry applied on metavolcaniclastics and metagranitoids and (4) $^{40}Ar/^{39}Ar$ dating of metamorphic white micas. Mineral chemistry of chlorite and phengite were performed with the electron probe microanalyser (EPMA) JEOL 8200 of the Università di Milano Statale "A. Desio", equipped with five wavelength-dispersive spectrometers. The point analyses were acquired using 15 KeV accelerating voltage, 5 nA specimen current and 30 s of dwell time for peaks and 10 s for background. Chlorite and phengite structural formulas were calculated assuming 14 and 11 anhydrous oxygens, respectively (Tab. 1).

Thermobarometry was performed on metapelites sampled in the Metavolcanic and Metavolcaniclastic Fm., and metagranitoids. For metapelites, P-T equilibrium conditions of chlorite-phengite couples related to the D1 and D2 phases were estimated with the ChlMicaEqui software (Lanari, 2012) based on the Vidal & Parra (2000) method (Supplementary Data 1). The results were compared with other thermometers (Cathelineau, 1988; Bourdelle & Cathelineau, 2015) and barometers (Bousquet et al., 2002; Dubacq et al., 2010). Termobarometry on metagranitoids was performed using classical calibrations of Cathelineau & Nieva (1985), Cathelineau (1988) and Massonne & Schreyer (1987). Metamorphic white micas related to the D2 phase were separated from three samples of metagranitoids at the Dipartimento di Scienze della Terra (Università di Pisa) and hand-picked in CNRS (Géoazur, Valbonne). The analytical procedures and raw data are listed in the supplementary materials.

Sample CMD101 was crushed and 200-315 µm size fraction was cleaned in ultrasonic bath. White micas were carefully handpicked under a binocular microscope to select only grains without evidence of alteration or inclusions. Selected grains were packaged in aluminum foils and were irradiated for 97 h in the McMaster Nuclear Reactor (McMaster University, Ontario) together with Fish Canyon sanidine grains as flux monitor (28.030 ± 0.056 Ma, Jourdan & Renne, 2007). The argon isotopic interferences on K and Ca were determined by the

irradiation of KF and CaF2 pure salts from which the following correction factors were obtained: (^{40}Ar/^{39}Ar)K = 2.97 x 10-2 ± 10-3 at 1S, (^{38}Ar/^{39}Ar)K = 1,24 x 10-2 ± 5 x 10-4 at 1S, (^{39}Ar/^{37}Ar)Ca = 7.27 x 10-4 ± 4 x 10-5 at 1S, and (^{36}Ar/^{37}Ar)Ca = 2.82 x 10-4 ± 3 x 10-5 at 1S. ^{40}Ar/^{39}Ar step heating analyses were performed at Géoazur Nice (France) using a continuous 100 W PhotonMachine CO2 (IR) laser used at 5-15% during 30 s. Argon isotopes were measured in static mode using an ARGUS VI mass spectrometer from Thermo-Fischer. Measurements were carried out in multi-collection mode using four Faraday cups equipped with 1012 ohm (masses 40, 39, 38 and 37) and one low-background compact discrete dynode ion counter to measure mass 36. Collector gain calibration is performed by the computer-controlled application of predetermined voltages to each collector. Mass discrimination for the mass spectrometer was monitored by regularly analyzing air pipette volumes. The raw data (Supplementary data 2) were processed using the ArArCALC software (Koppers, 2002), and ages were calculated using the decay constants given by Steiger & Jäger (1977). Blanks were monitored after every three sample analyses. All parameters and relative abundance values are provided in supplementary data set and have been corrected for blanks, mass discrimination, and radioactive decay. Atmospheric ^{40}Ar was estimated using a value of the initial ^{40}Ar/^{36}Ar of 298.56 (Lee et al., 2006) Our criteria for the determination of a plateau are as follows: a plateau must include at least 70% of ^{39}Ar released, over a minimum of three consecutive steps agreeing at 95% confidence level. Plateau ages are given at the 2S error level, and the plateau age uncertainties include analytical and J-value errors. All the errors on the inverse isochron, total fusion ages, and initial ^{40}Ar/^{36}Ar ratios are quoted at the 2S error.

4 Results

The presence of a continental tectonic unit (i.e., Ghisoni Unit) belonging to the Lower Units in the study area (Figs. 1, 2) was recognized for the first time by Di Rosa and co-authors (Di Rosa et al., 2019a, 2020a, 2020c). These authors interpreted the portion of continental lithosphere cropping out between Venaco village and the Fium'Orbo valley as the northern portion of the Ghisoni Unit. In the light of the structural and metamorphic evidence collected in this work, however, this portion of the Ghisoni Unit is here re-interpreted as an independent tectonic unit, named Venaco Unit (VEU) (Fig. 1). VEU is bounded by two strike-slip faults belonging to CCFZ that separate it from the Hercynian Corsica, on the west, the Schistes Lustrés Complex (i.e., Inzecca and Bagliacone-Riventosa Units), toward east (Fig. 2). Its lower portion consist of by Permian metagranitoids and cut by mafic dykes (Fig. 3a, Di Rosa et al., 2020d) intruded into a poly-metamorphic rocks assemblage of Panafrican age (i.e., Roches Brunes Fm.; Figs. 3b, c, Rossi et al., 1994). This basement is covered by a Permian meta-volcano sedimentary succession (i.e., Metavolcanic and Metavolcaniclastic Fm., e.g., Di Rosa, 2021). The latter succession consists of thin to medium layers of metapelites, metasandstones and fine-grained metabreccias interlayered with volcanic lavas mainly represented by metarhyodacites (Figs. 2, 3d-f).

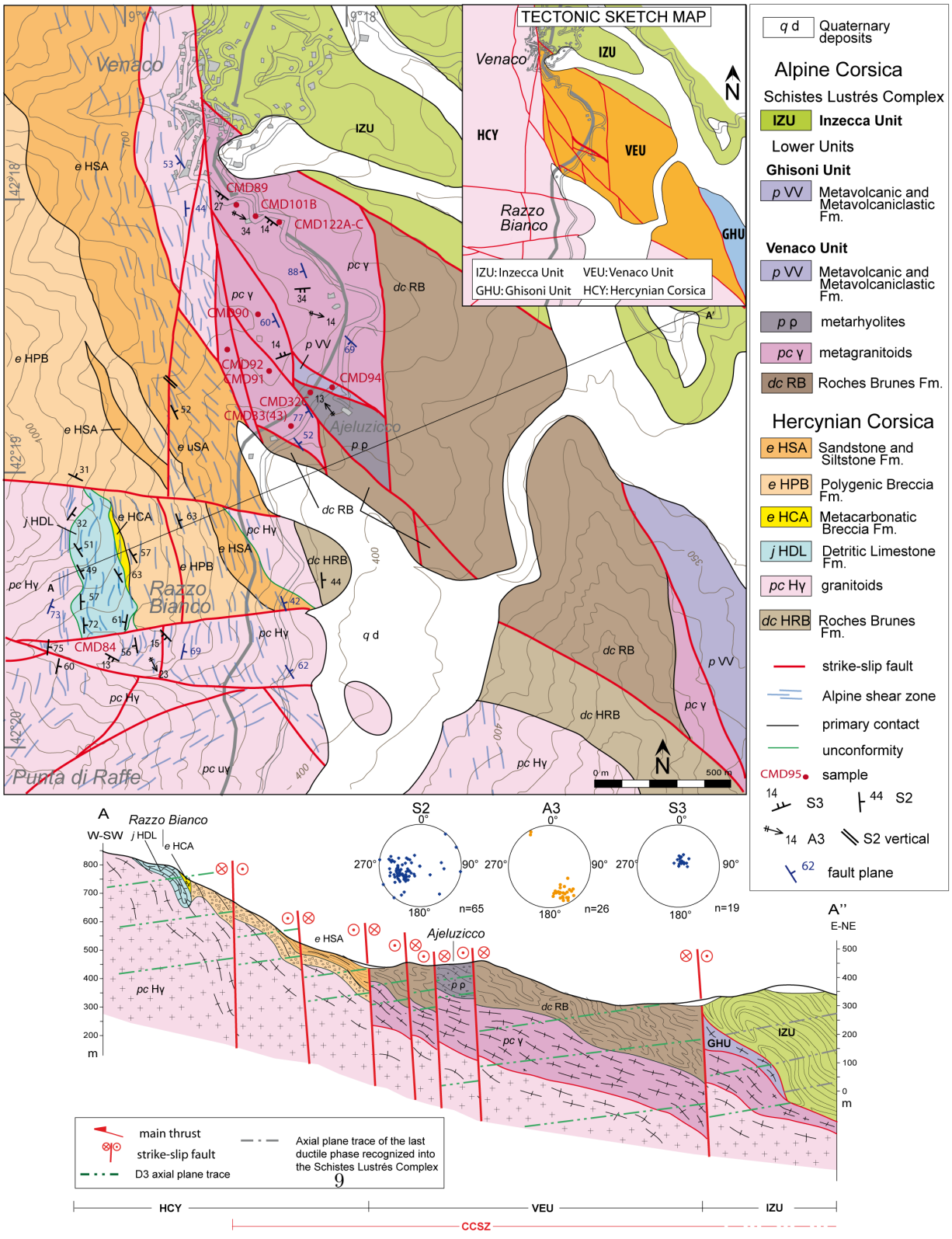
TECTONIC SKETCH MAP
Venaco
IZU
HCY
VEU
GHU
Razzo Bianco
IZU: Inzecca Unit
VEU: Venaco Unit
GHU: Ghisoni Unit
HCY: Hercynian Corsica
Venaco
IZU
e HSA
CMD89
CMD101B
CMD122A-C
pc γ
dc RB
CMD90
p VV
CMD92
CMD91
CMD94
CMD32C
CMD83(43)
Ajeluzicco
p ρ
e HPB
e HSA
e uSA
j HDL
e HCA
pc Hγ
e HSA
dc HRB
e HPB
Razzo Bianco
pc Hγ
CMD84
q d
dc RB
p VV
pc γ
dc HRB
pc Hγ
pc Hγ
Punta di Raffe
pc uγ
A
A'
N
0 m
500 m
q d Quaternary deposits
Alpine Corsica
Schistes Lustrés Complex
IZU Inzecca Unit
Lower Units
Ghisoni Unit
p VV Metavolcanic and Metavolcaniclastic Fm.
Venaco Unit
p VV Metavolcanic and Metavolcaniclastic Fm.
p ρ metarhyolites
pc γ metagranitoids
dc RB Roches Brunes Fm.
Hercynian Corsica
e HSA Sandstone and Siltstone Fm.
e HPB Polygenic Breccia Fm.
e HCA Metacarbonatic Breccia Fm.
j HDL Detritic Limestone Fm.
pc Hγ granitoids
dc HRB Roches Brunes Fm.
strike-slip fault
Alpine shear zone
primary contact
unconformity
CMD95 sample
S3
S2
A3
S2 vertical
fault plane
A
Razzo Bianco
W-SW
j HDL
e HCA
e HSA
Ajeluzicco
pc Hγ
p ρ
dc RB
pc γ
GHU
IZU
m
A''
E-NE
S2
A3
S3
n=65
n=26
n=19
main thrust
strike-slip fault
D3 axial plane trace
Axial plane trace of the last ductile phase recognized into the Schistes Lustrés Complex
HCY
VEU
IZU
CCSZ

Figure 2. Figure 2. Geological map, tectonic sketch, cross section and stereographic projections of Venaco Unit. In the sketch, HCY: Hercynian Corsica; VEU: Venaco Unit; GHU: Ghisoni Unit; IZU: Inzecca Unit.

4.1 Mesostructures of VEU

VEU shows a polyphase deformation composed by three ductile events (D1-D3 phases) like those described for GHU by Di Rosa et al. (2019a). In this work, unpublished data regarding the mesoscopic structural analyses are presented.

Relics of D1 phase (S1 foliation) was exclusively documented in the hinge zones of the F2 folds within fine-grained metasandstone and metapelites belonging to the Metavolcanic and Metavolcaniclastic Fm. The main structures documented in all the lithotypes can be assigned to D2 phase. In the metapelites, this phase produced F2 isoclinal folds with SSE-NNW trending A2 axis plunging less than 30° toward SE and an S2 axial plane foliation bearing a mineral and stretching L2 lineation trending ESE-WNW (Fig. 2). In the F2 hinge zones, it is a spaced crenulation cleavage. The S2 foliation strikes NNW-SSE with variable dip due to the later D3 folding phase.

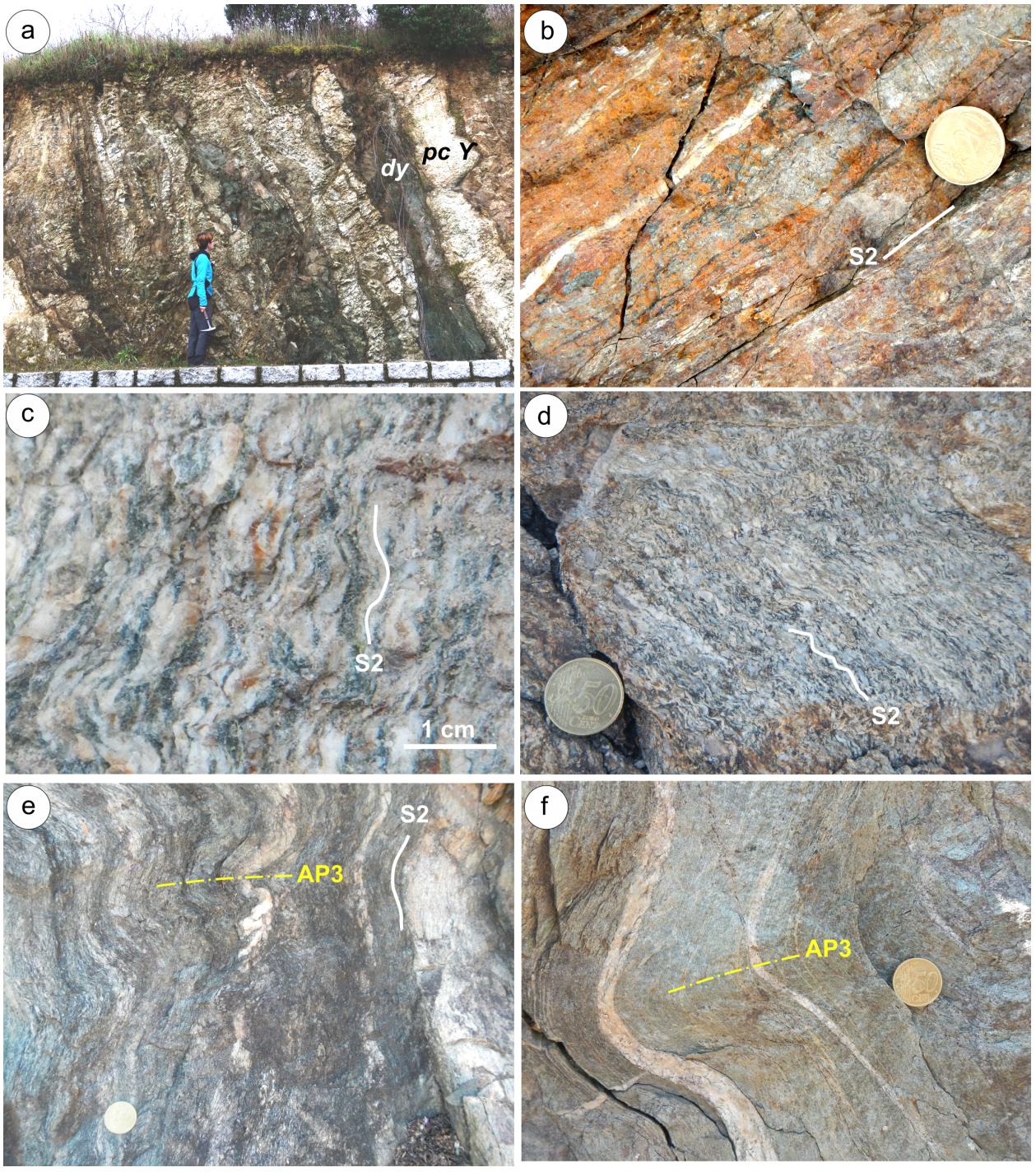

Figure 3. Mesoscopic deformation and lithotypes of Venaco Unit. (a)

Metagranitoids hosting mafic dyke; (b) Roches Brunes Fm., the S2 foliation trend is shown; (c) S2 foliation in metagranitoids; (d) metarhyolites showing the S2 foliation; (e) Metavolcanics and Metavolcaniclastic Fm. showing the S2 foliation, F3 fold and related axial plane foliation (AP3) and (f) F3 fold and related axial plane foliation into the Metavolcanics and Metavolcaniclastic Fm..

The metagranitoids show protomylonitic to ultramylonitic fabrics (Passchier & Trouw, 2005) with a S2 mylonitic foliation wrapping centimeter-sized quartz and feldspars grains showing strong shape preferred orientation and high aspect ratio (long axis/short axis: 13:3 and 9:3). The intrusive contact between metagranitoids and mafic dykes, even if locally deformed by F2 isoclinal folds, is mainly parallel to the S2 foliation documented in the metagranitoids (Fig. 3a). A pervasive feature of the metagranitoids and Metavolcanics and Metavolcaniclastics Fm. is represented by syn-D2 quartz veins trending parallel to the S2 foliation (Figs. 3e, f).

The last ductile phase (D3) was documented in the Metavolcanic and Metavolcaniclastic Fm. It produced open to close F3 asymmetric folds with sub-horizontal NW-SE trending A3 axes and S3 spaced axial plane foliation gently dipping to WSW (Figs. 2, 3e, f). The interference between F2 and F3 fold produced type 3 interference pattern (Ramsay, 1967). F3 folds affect the entire Hercynian Corsica-VEU- Schistes Lustrés Complex tectonic stack, constraining their coupling to before the D3 phase.

The last event documented in the field is responsible of the current architecture of the unit (Fig. 2). It produced high-angle sinistral strike-slip faults and secondary low-angle sinistral and high-angle dextral fault systems (i.e., the CCFZ) which activity was responsible of the exhumation of VEU from ductile-brittle transition up to the present-day position, as described for GHU by Di Rosa et al. (2019a).

4.2 Microstructures of VEU

Metapelites were sampled on the Metavolcanic and Metavolcaniclastic Fm. cropping out along the road T20 south of Venaco (sample CMD94, Fig. 2). In the metapelites, S1 foliation preserved in D2 microlithons, is a continuous, coarse-grained schistosity marked by the syn-kinematic growth of chlorite, phengite, albite, quartz with minor k-feldspar and calcite (Figs. 4a, b). Chlorite and phengite related to the D1 phase reach 400 µm in length. The metamorphic minerals association grown during the D2 phase includes chlorite, white mica and quartz (Fig. 4b). D2 phase chlorite and phengite do not exceed 100 µm in length. At the microscale, the S3 foliation in metapelites is classifiable as a spaced crenulation cleavage associated with minor recrystallization of calcite and quartz.

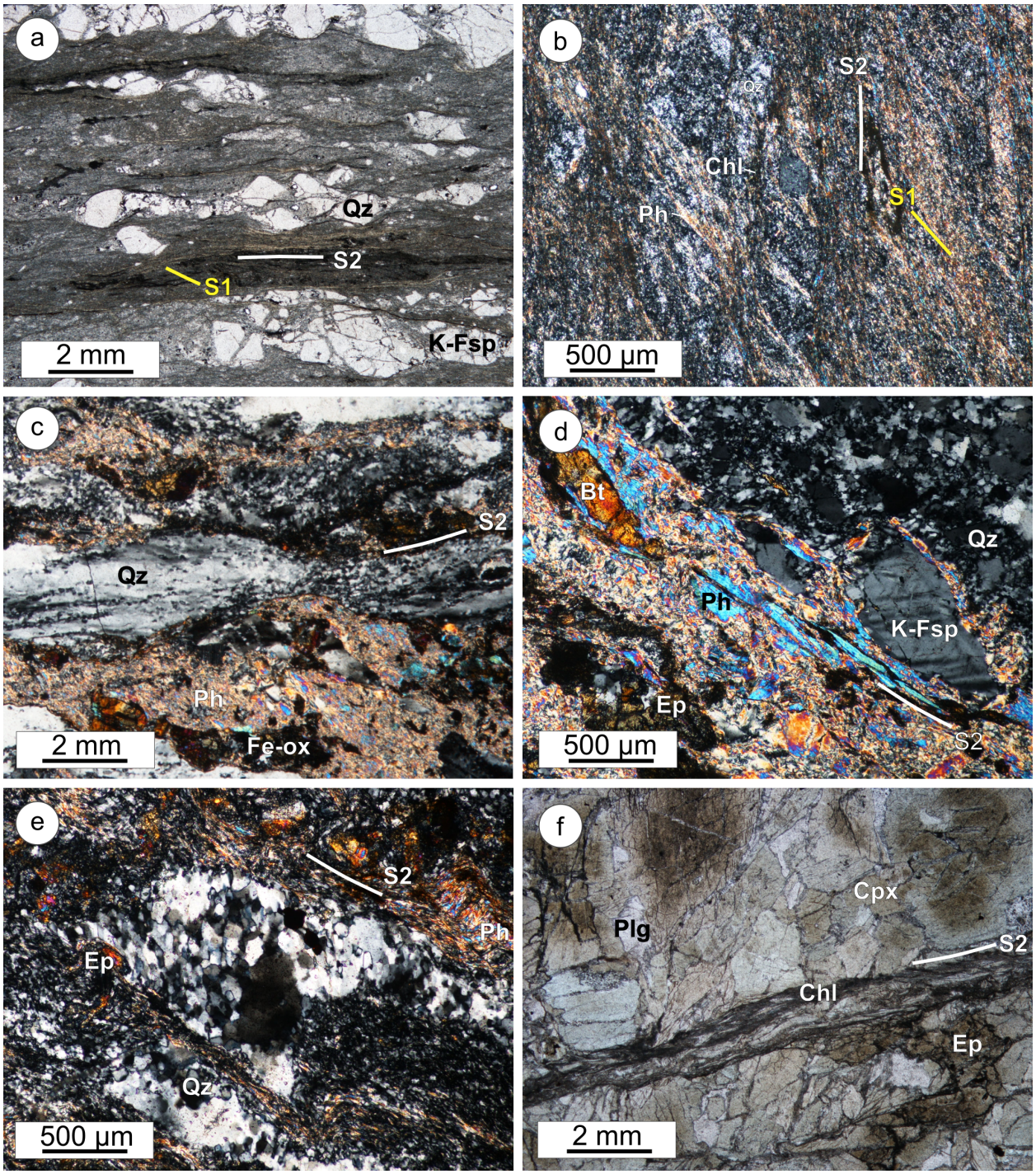
a
Qz
S2
S1
K-Fsp
2 mm
b
Qz
S2
Chl
Ph
S1
500 µm
c
S2
Qz
Ph
Fe-ox
2 mm
d
Bt
Qz
Ph
K-Fsp
Ep
S2
500 µm
e
S2
Ph
Ep
Qz
500 µm
f
Cpx
Plg
S2
Chl
Ep
2 mm

Figure 4. Microscopic features of the Venaco Unit. (a) S2 foliation in the Metavolcanics and Metavolcaniclastic Fm., sample CMD94; (b) S1-S2 foliations in the Metavolcanics and Metavolcaniclastic Fm., sample CMD32C (c) Sub-grain rotation recrystallization mechanism in boudinated quartz vein, marking the S2 foliation in metagranitoids. The nacking of the vein and the S2 foliation are well shown, sample CMD92; (d) white mica crystals grown along the S2 foliation into metagranitoids, sample CMD92; (e) sub-grain rotation fabric in metagranitoids, sample CMD122A and (f) µ-shear zone parallel to the S2 foliation into the mafic dyke, sample CMD122B. Qz: quartz; Chl: chlorite; Ph: phengite, Fe-ox: iron oxides; Bt: biotite; Ep:epidote; K-Fsp: K-feldspar; Cpx: clinopyroxene.

At the thin section scale, the metagranitoids appear as pink biotite-bearing gneisses with monzogranitic compositions (i.e., suite U3 of Rossi et al., 2015) containing quartz, sanidine, albite, chlorite (that replace the former magmatic biotite), white mica, k-feldspar and minor epidote (Figs. 4c-e). Accessory minerals are zircon, allanite, apatite and titanite. The original magmatic texture is almost completely overprinted by the D2 shearing deformation. The S2 foliation shows mylonitic to ultramylonitic fabric marked by discontinuous layers of white mica + chlorite ± biotite and fine-grained recrystallized quartz + k-feldspar + albite wrapping cm-grained albite, plagioclase, and quartz porphyroclasts (Figs. 4c-e). The size of the white mica ranges between 200 and 400 µm. The microstructural data related to the metagranitoids of VEU (samples CMD92, CMD101b, CMD122A, Fig. 2) such as feldspar porphyroclasts (asymmetric tails, bookshelf structures) and the intracrystalline deformation of quartz (undulatory extinction, deformation bands, sub-grain rotation) corroborate the estimated deformation temperatures of 300-400 °C estimated for GHU by Di Rosa et al. (2019a). The only structures related to the D3 phase are represented by microfolds affecting the phyllosilicate-rich layers.

The mafic dyke is composed of clinopyroxene, plagioclase, amphibole, and less abundant quartz, opaque oxides, and epidote (Fig. 4f). The S2 mylonitic to ultramylonitic foliation is marked by an increase in intensity of foliation and a gradual decrease in size of clinopyroxene and plagioclase porphyroclasts, which however preserve asymmetric tails indicating a top-to-W sense of shear (Fig. 4f). Clinopyroxene are sometimes fractured and locally replaced by chlorite and plagioclase (Di Rosa et al., 2020d). The intrusive magmatic contact between mafic dyke and metagranitoids is marked by the presence of large crystal (up to 250 µm) of allanite hosted by the metagranitoid, which appear fractured and filled by epidote and of apatite.

4.3 Mineral chemistry of chlorite and phengite

Syn-kinematic chlorite and phengite crystals were selected in the metapelite and metagranitoid within structural sites related to the D1 (i.e., the S1 foliation) and the D2 phases (i.e., the S2 foliation).

	Metapelites (sample CMD94)	*Metagranitoids (sample CMD122)*			
	S1 foliation	*S2 foliation*	*S2 foliation*		
Chl analyse	*Chl9*	*Phg31*	*Chl7*	*Phg30*	*Chl*
Wt%					
SiO_2	29.33	53.03	28.95	48.65	28.8
TiO_2	0.08	-	-	-	0.01
Al_2O_3	19.80	25.58	20.28	29.86	19.9
FeO	20.44	2.91	20.72	1.63	20.9
MnO	0.32	0.026	0.32	-	0.27
MgO	18.59	3.51	18.6	1.84	18.0
CaO	0.29	0.07	0.13	0.02	0.31
Na_2O	0.01	0.01	0.02	0.08	0.04
K_2O	0.08	9.95	0.02	10.53	0.03
tot.	88.93	95.09	89.04	92.61	88.4
Cations					
Si	2.95	3.53	2.91	3.32	3.14
Al^{IV}	1.05	0.47	1.09	0.68	1.15
Al^{VI}	1.30	1.53	1.31	1.73	1.41
Ti	0.01	-	-	-	-
Fe^{tot}	1.72	0.16	1.74	0.09	1.90
Mn	0.03	-	0.03	-	0.03
Mg	2.79	0.35	2.79	0.19	2.92
Ca	0.03	0.01	0.01	-	0.04
Na	-	-	-	0.01	0.01
K	0.01	0.84	-	0.92	0.01
sum ox	14	11	14	11	14

Table 1: Representative EPMA analysis

In metapelite (CMD94), chlorites grown along the S1 foliation are characterized by Si and Al contents ranging between 2.93-3.23 and 2.23-2.38 atom per formula unit (a.p.f.u., Tab. 1), respectively, and by an XMg slightly higher than 0.50, indicating a predominance of the clinochlore end-member Fig. 5a). Within the compositional space, which includes chlorite having Si content higher than 3 a.p.f.u. (e.g., Inoue et al., 2009), these low-Al chlorites are arranged nearby the solid solution between sudoite and clinochlore + daphnite end-members. Having Si content of around 3 a.p.f.u., the total content of Mg and divalent Fe occupying the M1-M4 octahedral sites greater than 3.5 a.p.f.u. implies that the vacancies of D1 phase chlorite do not exceed 0.50 a.p.f.u. (Fig. 5a). A second chlorite generation crystallized along the S2 foliation has been found (Fig. 4b). Its Si content (always higher than 3.10 a.p.f.u.) differ from the Si content of D1 phase chlorite (Fig. 5a). D1 and D2 phase chlorite have instead similar Al, Fe^{2+}+Mg^{2+} contents and XMg, which determine also for this second generation an affinity for the clinochlore and-member and a vacancies content, which never exceed 0.5 a.p.f.u. (Fig. 5a).

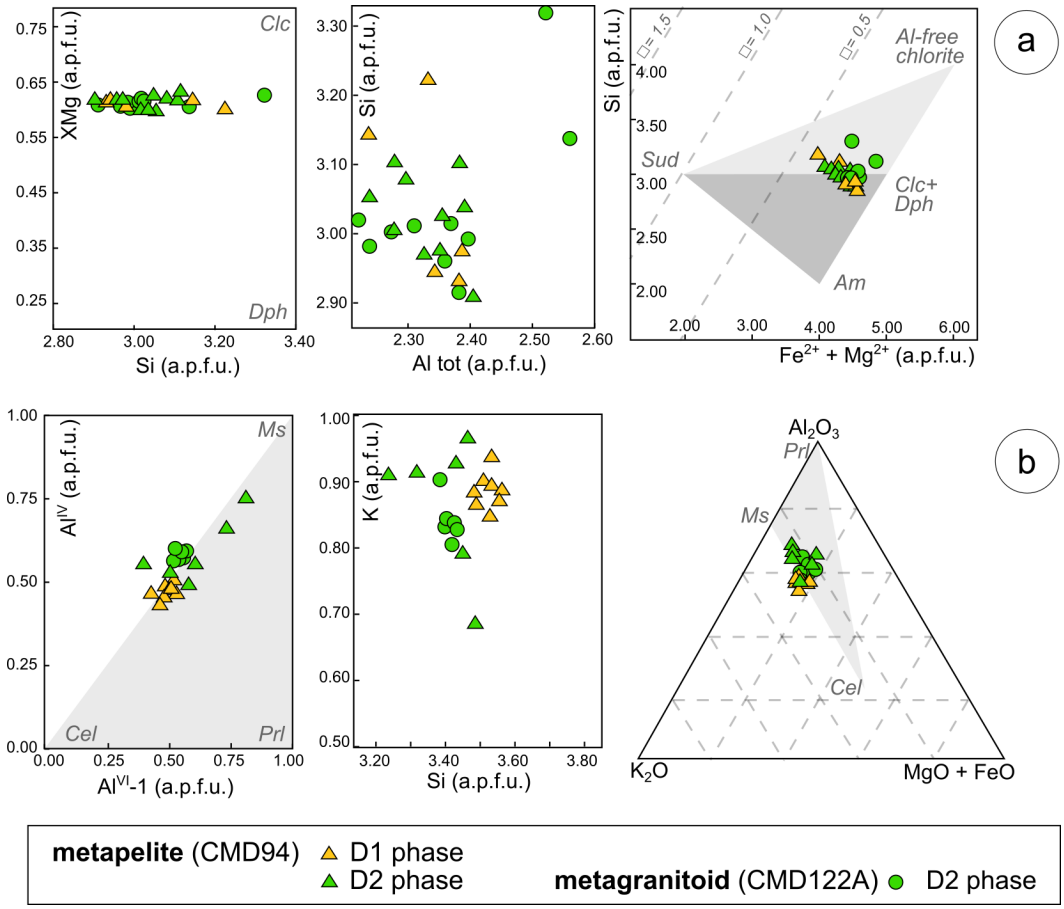

Figure 5. Mineral chemistry of (a) chlorite and (b) phengite found along the S1 and S2 foliations of the metapelite sample CMD94 and along the S2 foliation of the metagranitoid sample CMD122. In (a): dark and pale grey triangles indicate the compositional spaces delimited by chlorite end-members, defined by Vidal & Parra (2000) and Inoue et al. (2009), respectively. Am: amesite, Clc: clinochlore, Dph: daphnite, Sud: sudoite, empty square: vacancies (a.p.f.u.). In (b): grey triangles in the Al^{VI}-1 vs. Al^{IV} and the ternary diagrams indicate the phengite solid solutions from Bousquet et al. (2002) and from Vidal & Parra (2000), respectively. Cel: celadonite, Prl: pyrophyllite, Ms: muscovite.

In metagranitoids (CMD122A), the analyzed chlorites are related to the D2 phase. They show a more variable content on Si and Al than those of the metapelites (2.91-3.32 and 2.22-2.56 a.p.f.u., respectively) which determine a greater variability of the end-members proportion. However, also these chlorites tend to be magnesian (Fig. 5a).

Phengite have been found along the S1 and S2 foliations in metapelite (CMD94) and along the S2 foliation in metagranitoid (CMD122). All the analyzed phengites roughly plot along the perfect solid solution between celadonite and muscovite end-members, with those belonging to the D1 phase of the metapelite markedly tending toward the Al-poor end-member (Tab. 1 and Fig. 5b). D1 phase phengites are characterized by a very homogeneous composition, with moderately high Si content (3.50 a.p.f.u.) and K content between 0.85 and 0.95 a.p.f.u. (Fig. 5b). D2 phengites from metapelite have heterogeneous composition determining a wide range of end-member proportions, which however tends to the muscovite (Fig. 5b). The D2 phase phengites of the metagranitoid have Si (3.39-3.43 a.p.f.u.), K (0.81-0.09 a.p.f.u.) and Al (2.08-2.18 a.p.f.u.) contents like those of the D2 phengites from metapelites (Fig. 5b).

4.4 Thermobarometry on metapelite

Temperature and pressure estimate of the metapelite and metagranitoid were obtained using different methods (Figs. 6a-f). T in metapelites were calculated using on the composition of chlorite crystallized along the S1 and S2 foliations (CMD94). The calibrations of Cathelineau (1988) as well as those of Bourdelle & Cathelineau (2015) which includes the chlorites having Si content > 3 a.p.f.u., depict a wide thermal range where the chlorite of the D1 phase is in equilibrium (180-310 °C, Figs. 6a, b respectively) within which, however, a peak between 250-280 °C is clearly identified. Lower temperatures (< 225 °C) are related to chlorites having Si > 3 a.p.f.u. (Fig. 6b). Similarly, chlorites sampled along the S2 foliation seem to balance out at different temperatures (200-290 °C), but with a majority in the range 220-260 °C (Figs. 6a, b).

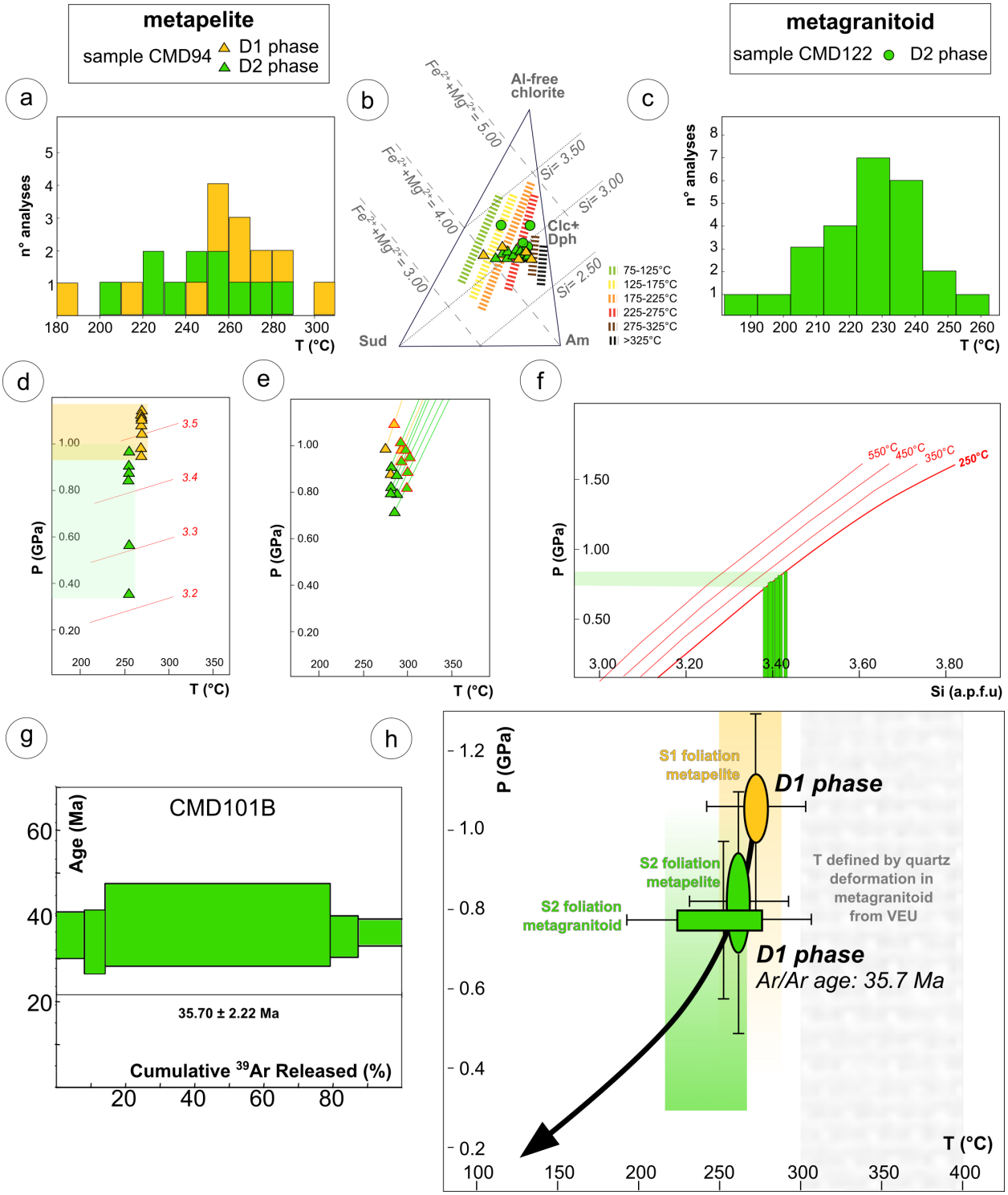
metapelite
sample CMD94
D1 phase
D2 phase
metagranitoid
sample CMD122
D2 phase
a
b
c
n° analyses
T (°C)
Al-free chlorite
Clc+ Dph
Sud
Am
Si= 3.50
Si= 3.00
Si= 2.50
75-125°C
125-175°C
175-225°C
225-275°C
275-325°C
>325°C
d
e
f
P (GPa)
T (°C)
Si (a.p.f.u)
550°C
450°C
350°C
250°C
g
h
CMD101B
Age (Ma)
35.70 ± 2.22 Ma
Cumulative ^{39}Ar Released (%)
S1 foliation metapelite
D1 phase
S2 foliation metapelite
S2 foliation metagranitoid
T defined by quartz deformation in metagranitoid from VEU
D1 phase
Ar/Ar age: 35.7 Ma

Figure 6. Thermobarometric results from metapelite and metagranitoid. (a) Chlorite-based thermometer, calibration of Cathelineau (1988); (b) chlorite-based thermometer, calibration of Bourdelle & Cathelineau (2015); (c) chlorite-based thermometer, calibration of Cathelineau & Nieva (1985); (d) phengite-based geobarometer, calibration of Bousquet et al. (2002). Red lines indicating Si content in phengite (a.p.f.u.); (e) Dubacq et al. (2010) calibration based on the water content in phengite. Calculations were performed fixing water activity to 0.9, % of Fe^{3+} to 0.32 of Fe_{tot} and the T to 260 and 250 °C for the D1 and D2 phases, respectively. Data rimmed in black and red indicate 95% or 93% of water, respectively. The reactions that define the equilibrium are (1) pyrophyllite = pyrophylliteH + water, (2) 3 Mg-celadonite + 4 pyrophyllite = 11 alpha-quartz + 2 muscovite + phlogopite + 2 pyrophylliteH, (3) 3 Mg-celadonite + 2 pyrophyllite = 11 alpha-quartz + 2 muscovite + phlogopite + 2 water and (4) 3 Mg-celadonite + 2 pyrophylliteH = 11 alpha-quartz + 2 muscovite + phlogopite + 4 water; (f) phengite-based geobarometer, calibration of Massonne & Schreyer (1987). (g) $^{40}Ar/^{39}Ar$ age spectra as a function of ^{39}Ar released. The error boxes of each step are at the 2S level. The error of ages is given at the 2S level. Ages were calculated using the ArArCalc software (Koppers, 2002) Raw data are presented in Supplementary Data 2. (h) Synthesis of the P-T-t conditions obtained from metapelite and metagranitoid of VEU in the area south of Venaco (D1 and D2 VEU).

Pressure equilibrium conditions during the D1 and the D2 phases were calculated by using Si in phengite calibration (Bousquet et al., 2002, Fig. 6d) and with the phengite-quartz-water method (Dubacq et al., 2010, Figs. 6e, g). In both cases, the calculations were obtained by fixing the T value to 260 °C (D1 phase) and 250 °C (D2 phase) resulting from the temperature previously estimated. Si in phengite allowed to constrain the P ranges of the D1 phase to 0.90-1.10 GPa and of the D2 phase to 0.35-0.95 GPa (Fig. 6d). A less dispersed result is obtained with the Dubacq's calibration (2010, Fig. 6e) which was obtained fixing the water activity to 0.9, compatible with the calcite content of the metapelite (for details see also Frassi et al., 2022) and admitting only the pressure conditions for which the optimal water content (in this case 93-95%) is the same for the greatest amount of analysis. By comparing the results, we can identify two peaks that are 0.90-1.10 GPa for the D1 phase and 0.70-1.00 GPa for the D2 phase. We were not able to obtain satisfactory P-T estimates with the chlorite-phengite-quartz-water method of Vidal & Parra (2000), since no phengite-chlorite couple was able to equilibrate with energy conditions below 1000 J.

4.5 Thermobarometry on metagranitoids

Temperature conditions related to the D2 phase of the metagranitoid (sample CMD122A) were calculated using two calibrations. Applying the calibration of

Bourdelle & Cathelineau (2015, Fig. 6b), our data are included in the T range of 125-325 °C. Less dispersed are the results obtained by applying the Cathelineau & Nieva (1985) thermometer (180-260 °C), based on the Al^{IV} content of chlorite (Fig. 6c). However, with both the calibrations a peak between 225 and 275 °C could is identified.

Microstructures in quartz and feldspar described in section 4.2, indicate that dislocation creep represents the main deformation mechanism in quartz during the development of the main foliation, suggesting deformation temperature of 300-400 °C (Stipp et al., 2002). Microstructures in feldspar suggest deformation temperature of 400-450 °C (Passchier & Trouw, 2005).

Pressure conditions of the D2 phase of the metagranitoid were obtained applying the Massonne & Schreyer (1987) calibration based on the Si content in phengite, assuming a fixed temperature value of 250 °C. Most of the phengite analysis yield P values of 0.75-0.80 GPa (Fig. 6f).

4.6 $^{40}Ar/^{39}Ar$ dating

As documented in section 4.3, the pervasive structure documented in the metagranitoids is the S2 foliation. No evidence of D1 domains or chlorites/phengites composition comparable to those grown along the S1 in metapelites were documented in metagranitoids samples. Metagranitoids represent so the ideal lithotype that should be used to constrain the age of S2 foliation. For this reason, a metagranitoid sample (CMD101b) poorly weathered and collected far from both D2 shear zones and cataclastic zones of CCFZ, were selected to obtain a metamorphic white mica separate used for single grain ^{40}Ar-^{39}Ar step-heating analysis. A single white mica grain yielded a plateau age of 35.7 ± 2.22 Ma, which corresponds to 100% of ^{39}Ar released and to 5 steps. The inverse isochron for the plateau steps provides a concordant age at 35.25 ± 3.89 Ma. An age of 35.7 ± 2.22 Ma can be considered as the most accurate age (Fig. 6g).

5 Discussion

5.1 P-T-d-t path of VEU

Linking the P and T conditions obtained using the chlorites and phengites grown along the S1 and S2 foliation a P-T-d path of VEU can be constructed (Figs. 6h, 7). The P-T conditions of 0.9-1.10 GPa and 260 °C for the D1 phase have been calculated from metapelites (sample CMD94) using the chlorites and phengites recrystallized along the S1 foliation. Due to the lack of evidence for an older relic foliation, the D1 phase can be regarded as the deformation event during which VEU reaches its maximum depths, 33 km (Fig. 6h). We have also identified a second P-T event recorded by the chlorites and phengites crystallized along S2 foliation in metapelites which constrain the P and T conditions of the D2 phase at 0.70-1.00 GPa and 250 °C. These data are coherent with the P-T estimates for the D2 phase obtained in metagranitoids (i.e., 0.75-0.80 GPa and 225-275 °C). Overall, all the collected data indicate that the D2 phase developed during a retrograde path at 26 km of depth (Fig. 6h).

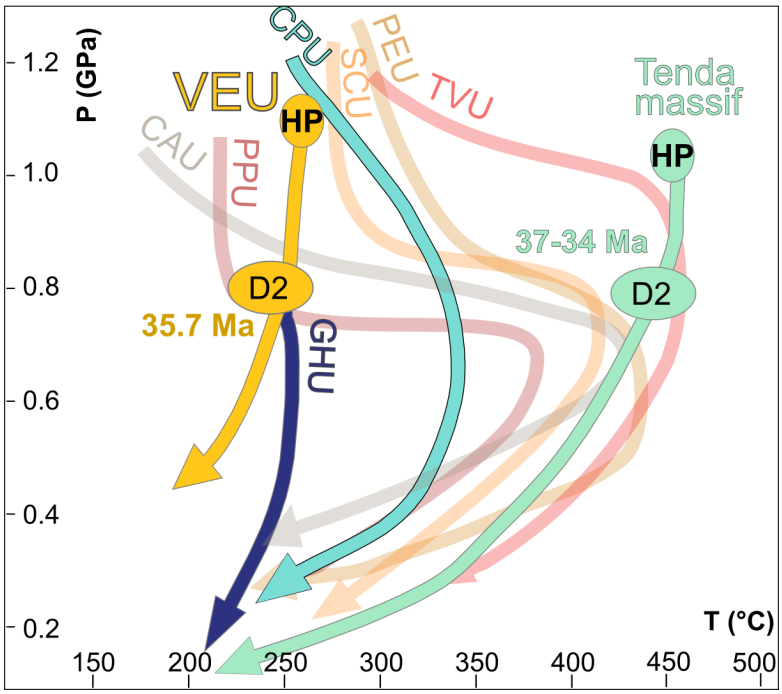

Figure 7. (a) The P-T-d conditions of VEU compared with the other Lower Units. From the Fium'Orbo area: Ghisoni Unit (GHU, from Di Rosa et al., 2019a). From Corte area: Castiglione-Popolasca (CPU), Piedigriggio-Prato (PPU) and Tour de Valletto (TVU) Units (Di Rosa et al., 2019a; Frassi et al., 2022). From Cima Pedani area: Canavaggia (CAU), Scoltola (SCU) and Pedani (PEU) Units (Di Rosa et al., 2019b). Tenda Massif path is taken from Molli et al. (2006).

Temperatures obtained for the D2 phase using microstructure- and petrology-based thermometers in metagranitoids is apparently in contrast. The activity of chlorite end-members as well as Al^{IV} in chlorite thermometers applied to the chlorite analysis of the metagranitoid (sample CMD122) indicates a temperature of max. 275 °C, whereas microstructures of quartz and feldspar indicate deformation temperatures of about 400 °C (Figs. 6c, f and h). This discrepancy, already described by Di Rosa et al. (2020c) for GHU in the Fium'Orbo valley, could be reduced including the error of 20 °C associated to the quantitative methods used to determine the T (e.g., Bourdelle & Cathelineau, 2015). In addition, since the metagranitoids are affected by syn-D2 veins systems, we suppose that the process of hydrolytic weakening was cyclically activated producing the overestimation of the deformation temperature (Law, 2014). We can so propose a reliable T range for the D2 phase registered by VEU between 270-280 °C.

The geothermal gradient of 7 °C/km calculated for VEU using the recommenda-

tion of Best (2003) is comparable to those obtained from P-T-d paths of other Lower Units (Di Rosa et al., 2017a, 2019a, 2019b, 2020b, 2020c; Frassi et al., 2022). The P-T-d path obtained for the VEU however indicates that the exhumation of the unit occurred under isothermal conditions (Fig. 7). The 'shape' of its retrograde path is however similar to the retrograde path of Castiglione-Popolasca and Ghisoni units (i.e., Lower Units located immediately above the Hercynian Corsica). For these units, the retrograde isothermal path can be explained assuming a fast exhumation stage during which the temperature peak does not exceed the temperature achieved at pressure peak (e.g., Di Rosa et al., 2019a), up to shallow structural levels. Conversely, most of the Lower Units show a warmed path (i.e., Croce d'Arbitro, Piedigriggio-Prato, Canavaggia, Pedani, Scoltola and Tour de Valletto units) during which the exhumation of continental units occurred together with a substantial (> 100 °C) increase of temperature (e.g., Frassi et al., 2022).

Moreover, it is important to underline that the $^{40}Ar/^{39}Ar$ dating of VEU was performed on the phengite crystallized on the S2 foliation of the metagranitoids. Considering that: (1) the temperature estimates from D2 syn-kinematic chlorites and phengites of VEU are below the supposed closing temperature of white micas (i.e., 350 °C: Hames & Bowring, 1994) and (2) the critical temperature for the total reset of the Ar is 260 °C (Hunziker, 1986), we consider the isotopic ages obtained for syn-kinematic white mica of the VEU to be valid and reliable.

In VEU, as well as in the other Lower Units, the exhumation-related tectonics continued during the D3 phase (Jolivet et al., 1991; Fournier et al., 1991; Daniel et al., 1996; Zarki-Jakni et al., 2004; Di Rosa et al., 2020a). No thermobarometric estimates are available for this phase because of the lack of phyllosilicates crystallizations along the S3 foliation. According to the map-scale structures geometrical relationships (Di Rosa et al., 2017b; Malasoma et al., 2020), the D3 phase developed when the stack of units has already formed and contributes to the final exhumation of the Alpine Corsica. The ages obtained by apatite fission tracks, which range from 35-25 Ma in southern Hercynian Corsica to <25 Ma in central Hercynian Corsica (Danišik et al., 2007), testify this later extensional tectonics, probably driven by the progressive collapse of Alpine Corsica associated with rifting in the Ligurian-Provençal back-arc basin.

5.2 Metamorphism and age constrain: implications for Alpine Corsica

In the Alpine Corsica, the remnants of the European continental margin deformed and metamorphosed under HP metamorphic conditions have been identified in the Tenda Massif located in the northeastern Corsica within the Alpine Domain (Gibbons & Horak, 1984; Molli & Tribuzio, 2004; Tribuzio & Giacomini, 2002; Maggi et al., 2012) and in the Lower Units cropping out with a north-south trend along the boundary between Hercynian and Alpine Corsica (Bezert & Caby, 1988; Garfagnoli et al., 2009; Malasoma & Marroni, 2007; Malasoma et al., 2006; Di Rosa et al., 2017b, 2019a). In addition, evidence of Alpine deformation has been found also in the eastern rim of the Hercynian Corsica, along localized shear zones close to the boundary with the Alpine Corsica

(Amaudric du Chaffaut & Saliot, 1979; Rossi et al., 1994; Di Vincenzo et al., 2016; Di Rosa et al., 2020a).

Most of the geodynamic reconstructions (Malavieille et al., 1998; Brunet et al., 2000; Molli et al., 2006; Malasoma & Marroni, 2007; Molli, 2008; Maggi et al., 2012; Marroni et al., 2017; Beaudoin et al. 2017; Di Rosa et al., 2020b) indicate that the European continental margin was dragged downward in an east-dipping subduction zone during the Early Tertiary. It is during this stage that they acquired the HP metamorphic imprint.

The only available age constraints of this HP metamorphism were obtained from the East Tenda shear zone (Fig. 1), a crustal-scale ductile shear zone with a complex kinematics originated during the underthrusting of the Tenda Massif in the subduction zone (Molli et al., 2006) and reactivated in extensional regime during exhumation (e.g., Jolivet et al., 1990). The age of the underthrusting event is roughly constrained to Early Eocene (Ypresian) by Brunet et al. (2000) that indicate a maximum age of 46.6 ± 1.2 Ma by phengite $^{40}Ar/^{39}Ar$ geochronology and by Maggi et al. (2012) that provide for the same event a U-Pb rutile age of 54 ± 8 Ma. The available data indicate that the Tenda Massif was buried at a depth between 30 km and 40 km (Fig. 8a, Gibbons & Horak, 1984; Maggi et al., 2012; Molli et al., 2006; Molli & Tribuzio, 2004; Rossetti et al., 2015; Tribuzio & Giacomini, 2002). The ages of 34-37 Ma (Priabonian), reported by Vitale Brovarone & Hewartz (2013) and by Brunet et al. (2000) for the East Tenda shear zone, constrain the exhumation of the Tenda Massif at 25-30 km of depth (Molli et al, 2006). This picture is recently confirmed by Beaudoin et al. (2020), that constrain the end of burial and exhumation at ~ 34 and ~ 22 Ma (Priabonian and Aquitanian), respectively.

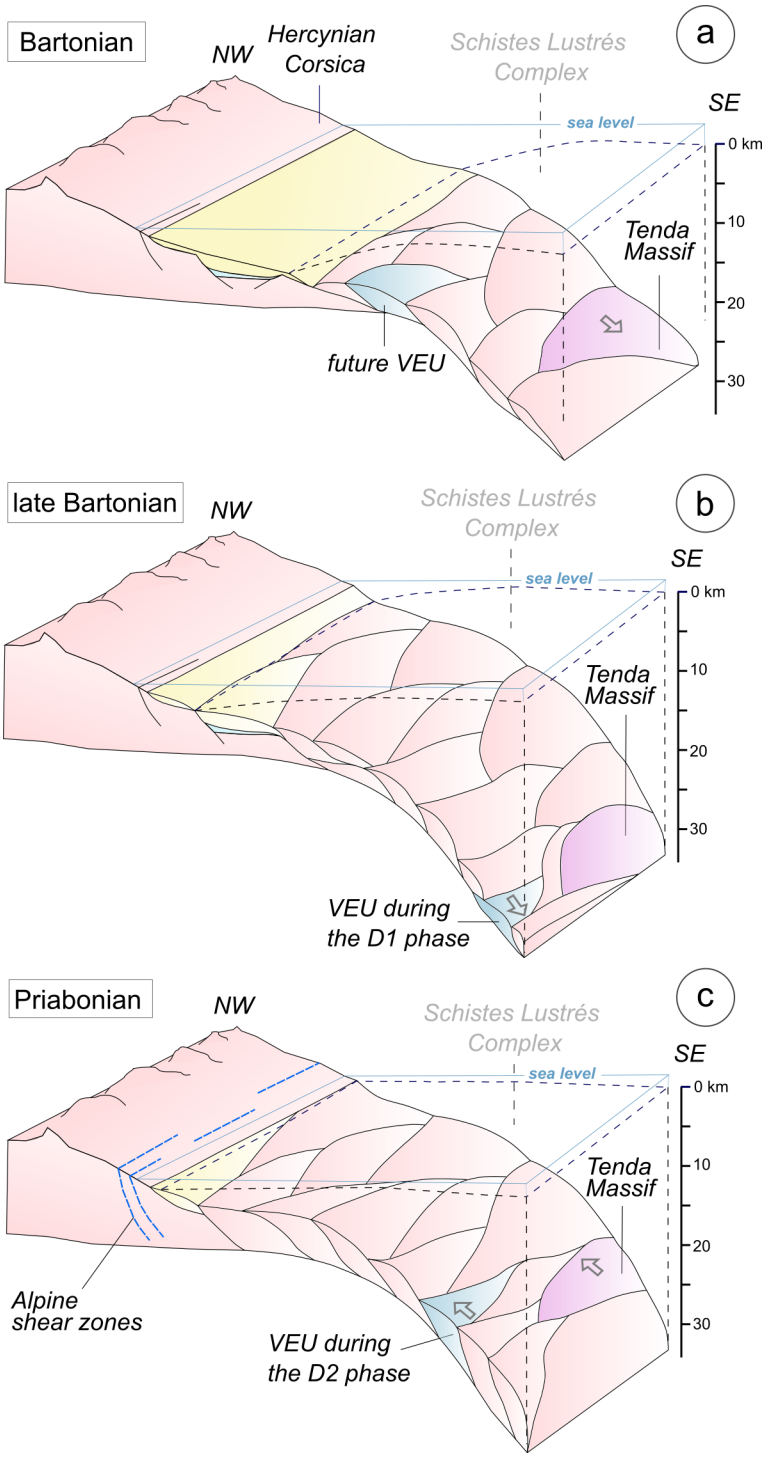
Bartonian
NW
Hercynian
Corsica
Schistes Lustrés
Complex
a
SE
sea level
0 km
10
20
30
Tenda
Massif
future VEU
late Bartonian
NW
Schistes Lustrés
Complex
b
SE
sea level
0 km
10
20
30
Tenda
Massif
VEU during
the D1 phase
Priabonian
NW
Schistes Lustrés
Complex
c
SE
sea level
0 km
10
20
30
Tenda
Massif
Alpine
shear zones
VEU during
the D2 phase

Figure 8. 3D sketch of the tectonic model related to the subduction of the European continental margin and the consequent exhumation of the resulting tectonic units in a still compressive setting. (a) The stage of subduction in the Bartonian: Tenda Massif is parked at 25-30 km of depth, VEU is next to the subduction and the foredeep deposits are settling on the margin. (b) During the late Bartonian, VEU is supposed to be at the maximum depth of 33 km and is deforming by the D1 phase while the Tenda Massif stands and heats up at 25-30 km. (c) In the Priabonian, VEU is quickly exhumed (D2 phase) and reach the Tenda Massif at about 26 km.

The others HP continental units (i.e., Lower Units) are characterized by a metamorphic sequence whose youngest deposits are represented by foredeep turbidites showing Bartonian microfossils in the uppermost stratigraphic levels (Bezert & Caby, 1988). This finding indicates that the underthrusting event and the related HP metamorphism probably occurred during the late Bartonian (i.e., after 41.2 Ma, Fig. 8b). This evidence is coherent with the metamorphism age of 35.7 Ma (Priabonian) that we obtained for the D2 event (i.e., the retrograde path) in the metagranitoids of VEU.

Alpine metamorphism was also found within top-to-the west shear zones occurring in the easternmost sector of the Hercynian Corsica (Rossi et al., 1994; Di Rosa et al., 2017b; Malasoma et al., 2020). The dating of these shear zones (Di Vincenzo et al., 2016) indicate for the Alpine metamorphism a minimum age of 46 Ma by $^{40}Ar/^{39}Ar$ analyses of white micas. As discussed by Di Rosa et al. (2020a) the age detected for these shear zones are in contrast with the Lutetian-Bartonian age of metabreccias and metasandstones affected by shear deformation. More reliable ages for the involvement of the Hercynian Corsica in the continental subduction have been obtained by the analyzed syn-shear white mica whose ages range between 37 and 35 Ma (Priabonian, Fig. 8c). Re-equilibration during exhumation at 33-32 Ma (Rupelian) is also suggested by these authors. The latter age has been interpreted by Di Rosa et al. (2020a) as developed during the exhumation of the eastern rim of the Hercynian Corsica.

These data can be framed into a coherent picture where the age of HP metamorphism achieved by the continental crust fragments during the underthrusting is progressively younger moving from northeast to southwest: Ypresian in the Tenda Massif, Bartonian in the Lower Units and probably Priabonian or younger in the westernmost rim of the Hercynian Corsica. The available data and those here presented, indicate the Lower Units and the Tenda massif were subducted at different times but at 34-36 Ma (Priabonian) are at the same depth of the exhumation path. At the same time, the westernmost rim of Hercynian Corsica was deformed by the top-to-the west shear zones according to the picture provided by Di Rosa et al. (2020a).

5.3 Geodynamic implications

To reconstruct the progressive involvement of the thinned European continental

margin in the east-dipping subduction zone, we compare the age of metamorphism here presented for the VEU (i.e., Lower Units) with those available for the continental unit of the Tenda Massif (the only continental unit of Alpine Corsica with isotopic age constraints; Brunet et al., 2000; Maggi et al., 2012). The involvement of the continental crust in the subduction zone followed the underthrusting of the last portion of the Ligure-Piemontese oceanic crust. The data available for the Internal Ligurian Units (i.e., the best-preserved fragments of the Ligure-Piemontese basins exposed along the Alpine Corsica - Northern Apennines transect) indicate that in the early Paleocene, some portions of oceanic crust were not yet involved in the subduction zone (Marroni, 1991; Molli, 2008; Marroni et al., 2017; Meneghini et al., 2020). The first sector of continental crust involved in the subduction zone was probably the sector currently represented by the Tenda Massif (i.e., the continental fragment showing the oldest HP metamorphic imprint). The involvement of the continental crust continued with the underthrusting of the more internal areas of the European margin, today represented by the Lower Units. Subsequently, also the westernmost rim of the Hercynian Corsica is involved in the same subduction zone.

The data available and those provided in this paper suggest that the Tenda Massif and the VEU (Lower Units) were dragged downward at different time (i.e., Ypresian for the Tenda Massif and Bartonian for the VEU) but both were exhumed simultaneously during the Priabonian. Consequently, these two units experienced different stationary time at depth, controlled by several boundary conditions as suggested by Frassi et al. (2022), like exhumation rate, exhumation trajectory, thermal state of the overriding plate and mechanical and rheological characteristics of the downgoing continental crust. The occurrence of European continental units characterized by different stationing time at depth has been described for the first time by Di Rosa et al. (2019a). According to these authors, the different stationing time at depth is correlated to the structural position within the subduction channel: the units with isothermal paths are located at the base of the subduction channel immediately over the Hercynian Corsica, whereas the units with warmed paths are located at its top, below the Schistes Lustrès Complex. Following this distinction, the P-T data related to the Tenda Massif, that experienced a warmed path (Molli & Tribuzio 2004), indicate that this continental slice experienced a long stationary time at depth before its exhumation. On the contrary, the data provided in this paper for the VEU indicate an isothermal path and then an exhumation predated by a short stationary time at depth.

6 Conclusion

In this paper, the P-T-d path of the VEU is reconstructed and combined to the $^{40}Ar/^{39}Ar$ dating of syn-kinematic muscovite to present the first P-T-d-t path of a Lower Units. The proposed scenario indicates that the VEU reached the baric peak (D1 phase) at 33 km of depth in the Bartonian time (post 41.2 Ma). At 35.7 Ma (middle Priabonian), VEU was exhumed at shallower structural level (26 km of depth) mainly through the activation the D2 top-to-the W shear

zones. The retrograde isothermal path of the VEU indicates that its stationary time at depth was minimum and that after reaching the maximum depth it is "quickly" exhumed.

The comparison of the new isotopic data presented in this contribution with the only one available for a continental unit (i.e., Tenda Massif) allows proposing a new scenario for the progressive involvement of the thinned European continental margin in the east-dipping subduction zone. This scenario includes the underthrusting of the continental fragments in different time and in different structural positions within the subduction channel of the alpine orogenic wedge. Each fragment underwent thus a different stationing time at depth, as indicated by the "shape" of the P-T-d path, and then started to be exhumed together within the subduction channel. This behavior can be proposed as effective for all the HP continental units during the continental subduction and must be thus considered to understand the alpine geodynamic history.

Acknowledgments

This work was supported by Prin 2020 resp. Michele Marroni. We thank the Nuclear Operation and Facilities of the McMaster University and Andrea Risplendente for the technical support during mica irradiation and microprobe analysis. We also thank *(editor)* and *(reviewers)* for the constructive reviews.

References

Alessandri, J. A., Magné, J., Pilot, M. D., & Samuel, E. (1977), Le Miocène de la région de Corte-Francardo. *Bulletin de la Société Scientifique de Histoire Naturelle de la Corse,* 622, 51-54.

Amaudric du Chaffaut, S., & Saliot, P. (1979), La region de Corte: sectèurclè pour la comprehension du métamorphisme alpine en Corse. *Bulletin de la Société Géologique de France,* 21, 149-154.

Amaudric du Chaffaut, S., Bonin, B., Caron, J. M., Conchon, O., Rossi, P., Bimbier, A., Damiani, L., Dominici, R., Heetveld, H., & Rouire, J. (1985), Carte Géologique de la France, feuille Venaco (1114). *BRGM*, scale 1 :50000, 1 sheet.

Beaudoin, A., Augier, R., Jolivet, L., Jourdon, A., Raimbourg, H., Scaillet, S., & Cardello, G. L. (2017), Deformation behavior of continental crust during subduction and exhumation: Strain distribution over the Tenda massif (Alpine Corsica, France). *Tectonophysics,* 705, 12–32. https://doi.org/10.1016/j.tecto.2017.03.023.

Beaudoin, A., Scaillet, S., Mora, N., Jolivet, L., & Augier, R. (2020), In Situ and step-heating 40Ar/39Ar Dating of white mica in Low-temperature shear zones (Tenda Massif, Alpine Corsica). *Tectonics,* 10.1029/2020TC006246.

Best, M. G. (2003), *Igneous and metamorphic petrology (2^{nd} ed.).* Oxford, Blackwell.

Bezert, P., & Caby, R. (1988). Sur l'age post-bartonien des événements tectonométamorphiques alpins en bordure orientale de la Corse cristalline (Nord de Corte). *Bulletin de la Société Géologique de France,* 4(6), 965-971.

Bill, M., Bussy, E., Cosca, M. A., Masson, H., & Hunziker, J. C. (1997), High precision U-Pb and 40Ar/39Ar dating of an Alpine ophiolite (Gets nappe, French Alps). *Eclogae Geologicae Helvetiae*, 90, 43 -54.

Bourdelle, F., & Cathelineau, M. (2015), Low-temperature chlorite geothermometry: a graphical representation based on a T–R2+–Si diagram. *European Journal of Mineralogy,* 27, 617-626.

Bousquet, R., Goffé, B., Vidal, O., Oberhaensli, R., & Patriat, M. (2002), The tectono-metamorphic history of the Valaisan Domain from the Western to the Central Alps: new constraints on the evolution of the Alps. *Geological Society of America Bulletin,* 114, 207-225.

Brunet, C., Monié, P., Jolivet, L., & Cadet, J. P. (2000), Migration of compression and extension in the Tyrrhenian Sea, insights from $^{40}Ar/^{39}Ar$ ages on micas along a transect from Corsica to Tuscany. *Tectonophysics,* 321, 127-155.

Cabanis, B., Cochemé, J. J., Vellutini, P. J., Joron, J. L., & Treuil, M. (1990), Post- collisional Permian volcanism in northwestern Corsica: an assessment based on mineralogy and trace-element geochemistry. *Journal of Volcanology and Geothermal Research*, 44, 51-67.

Caron, J. M., & Péquignot, G. (1986), The transition between blueschists and lawsonite-bearing eclogites based on observations from Corsican metabasalts. *Lithos,* 19 (3-4), 205-218.

Cathelineau, M. (1988), Cation site occupancy in chlorites and illites as a function of temperature. *Clay Minerals,* 23, 471-485.

Cathelineau, M., & Nieva, D. (1985), A chlorite solid solution geothermometer the Los Azufres (Mexico) geothermal system. *Contributions to Mineralogy and Petrology,* 91, 235-244.

Chopin, C., Beyssac, O., Bernard, S., & Malavieille, J. (2008), Aragonite-grossular intergrowths in eclogite-facies marble, Alpine Corsica. *European Journal of Mineralogy,* 20, 857-865.

Dallan, L., & Nardi, R. (1984), Ipotesi dell'evoluzione dei domini "liguri" della Corsica nel quadro della paleogeografia e della paleotettonica delle unità alpine. *Bollettino della Società Geologica Italiana,* 103, 515-527.

Daniel, J. M., Jolivet, L., Goffé, B., & Poinssot, C. (1996), Crustal-scale strain partitioning: footwall deformation below the Alpine Oligo-Miocene detachment of Corsica. *Journal of Structural Geology,* 18(1), 41–59.

Danišik, M., Kuhlemann, J., Dunkl, I., Székely, B,. & Frisch, W. (2007), Burial and exhumation of Corsica (France) in the light of fission track data. *Tectonics,* 26, TC1001. https://doi.org/10.1029/2005T C001938

Di Rosa, M., De Giorgi, A., Marroni, M., & Vidal, O. (2017a), Syn-convergence exhumation of continental crust: evidence from structural and metamorphic analysis of the Monte Cecu area, Alpine Corsica (Northern Corsica, France). *Geological Journal,* 52, 919-937.

Di Rosa, M., De Giorgi, A., Marroni, M., & Pandolfi, L. (2017b), Geology of the area between Golo and Tavignano Valleys (Central Corsica): a snapshot of the continental metamorphic units of Alpine Corsica. *Journal of Maps,* 13, 644-653.

Di Rosa M., Frassi C., Meneghini F., Marroni M., Pandolfi L., & De Giorgi, A. (2019a), Tectono-metamorphic evolution in the European continental margin involved in the Alpine subduction: new insights from the Alpine Corsica, France. *Comptes Rendus de Académié de Sciences Paris,* 351(5), 384-394.

Di Rosa, M., Meneghini, F., Marroni, M., Hobbs, N., & Vidal, O. (2019b), The exhumation of continental crust in collisional belts: insights from the deep structure of Alpine Corsica in the Cima Pedani area. *Journal of Geology,* 127(3), 263-288.

Di Rosa, M., Frassi, C., Marroni, M., Meneghini, F., & Pandolfi, L. (2020a), Did the "Autochthonous" European foreland of Corsica Island (France) experience Alpine subduction? *Terra Nova,* 32, 34-43.

Di Rosa, M., Meneghini, F., Marroni, M., Frassi, C., & Pandolfi, L. (2020b), The coupling of high-pressure oceanic and continental units in Alpine Corsica: evidence for syn-exhumation tectonic erosion at the roof of the plate interface. *Lithos,* 354-355, 105328.

Di Rosa, M., Frassi, C., Malasoma, A., Marroni, M., Meneghini, F., & Pandolfi, L. (2020c), Syn-exhumation coupling of oceanic and continental units along the western edge of the Alpine Corsica: a review. *Ofioliti,* 45(2), 71-102.

Di Rosa, M., Farina, F., Lanari, P., & Marroni, M. (2020d), Pre-Alpine thermal history recorded in the continental crust from Alpine Corsica (France): evidence from zircon and allanite LA-ICP-MS dating. *Swiss Journal of Geosciences,* 113, 19.

Di Rosa, M. (2021), *Tectono-metamorphic evolution of the continental units along the edge between Alpine and Hercynian Corsica.* Firenze University press.

Di Vincenzo, G., Grande, A., Prosser, G., Cavazza, W., & DeCelles, P.G. (2016), $^{40}Ar/^{39}Ar$ laser dating of ductile shear zones from central Corsica (France): Evidence of Alpine (middle to late Eocene) syn-burial shearing in Variscan granitoids. *Lithos,* 262, 369-383.

Dubacq, B., Vidal, O., & De Andrade, V. (2010), Dehydration of dioctahedral aluminous phyllosilicates: thermodynamic modelling and implications for

thermobarometric estimates. *Contributions to Mineralogy and Petrology,* 159, 159–174.

Durand-Delga, M., Peybernès, B., & Rossi, P. (1997), Arguments en faveur de la position, au Jurassique, des ophiolites de Balagne (Haute-Corse, France) au voisinage de la marge continentale européenne. *Comptes Rendus de l'Académie des Sciences,* 325, 973-981.

Durand-Delga, M. (1984), Principaux traits de la Corse Alpine et correlations avec les Alpes Ligures. *Memorie della Società Geologica Italiana,* 28, 285-329.

Elter, P., & Pertusati, P. (1973), Considerazioni sul limite Alpi-Appennino e sulle relazioni con l'arco delle Alpi Occidentali. *Memorie della Società Geologica Italiana,* 12, 359-375.

Faure, M., & Malavieille, J. (1981), Étude structurale d'un cisaillement ductile: le charriage ophiolitique corse dans la région de Bastia. *Bulletin de la Société Géologique de France,* 23(4), 335-343.

Favre, P., & Stampfli, G. M. (1992), From rifting to passive margin: the example of the Red Sea, Central Atlantic and Alpine Tethys. *Tectonophysics,* 215, 69-97.

Ferrandini, M., Ferrandini, J., Loye-Pilot, M. D., Butterlin, J., Cravatte, J., & Janin, M. C. (1998), Le Miocène du bassin de Saint-Florent (Corse): modalités de la transgression du Burdigalien supérieur et mise en évidence du Serravallien. *Geobio,* 31(1), 125-137.

Ferrandini, J., Ferrandini, M., Rossi, P., & Savary-Sismondini, B. (2010), Définition et datation de la formation de Venaco (Corse): dépot d'origine gravitaire d'age Priabonien. *Comptes Rendus de Geoscience,* 342, 921-929.

Fournier, M., Jolivet, L., Goffé, B., & Dubois, R. (1991), The Alpine Corsica metamorphic core complex. *Tectonics,* 10, 1173–1186.

Frassi, C., Di Rosa, M., Farina, F., Pandolfi, L., & Marroni, M. (2022), Anatomy of a deformed upper crust fragment from western Alpine Corsica (France): Insights into continental subduction processes. *International Geology Review.* https://doi.org/10.1080/00206814.2022.2031315

Froitzheim, N., & Manatchal, G. (1996), Kinematics of Jurassic rifting, mantle exhumation, passive margin formation in the Austroalpine and Penninic nappes (Eastern Switzerland). *Geological Society Annual Bulletin,* 108, 1120-1333.

Garfagnoli, F., Menna, F., Pandeli, E., & Principi, G. (2009), Alpine metamorphic and tectonic evolution of the Inzecca-Ghisoni area (southern Alpine Corsica, France). *Geological Journal,* 44, 191–210.

Gibbons, W., & Horak, J. (1984), Alpine metamorphism of Hercynian horneblende granodiorite beneath the blueschist facies Schistes Lustrés nappe of NE Corsica. *Journal of Metamorphic Geology,* 2, 95-113.

Gueydan, F., Leroy, Y. M., Jolivet, L., & Agard, P. (2003), Analyses of continental midcrustal strain localization induced by microfaultinf and reactionsoftening. *Journal of Geophysical Research,* 108, 2064-2081.

Guieu, G., Loye-Pilot, M. D., Lahondére, D., & Ferrandini, J. (1994), Carte géologique de France (1/50000), feuille Bastia (1111). *BRGM,* Orléans.

Hames, W. E., & Bowring, S. A. (1994), An empirical evaluation of the argon diffusion geometry in muscovite. *Earth and Planetary Science Letters,* 124(1), 161-169. Doi:10.1016/0012-821x(94)00079-4.

Handy, M. R., Schmid, S. M., Bousquet, R., Kissling, E., & Bernoulli, D. (2010), Reconciling plate–tectonic reconstructions of Alpine Tethys with the geological–geophysical record of spreading and subduction in the Alps. *Earth Science Review,* 102, 121–158.

Hunziker, J. C. (1986), The evolution of illite to muscovite: an example of the behavior of isotopes in low-grade metamorphic terranes. *Chemical Geology,* 57(1-2), 31-40.

Inoue, A., Kurokawa, K., & Hatta, T. (2009), Application of Chlorite Geothermometry to hydrothermal alteration in Toyoha Geothermal System, Southwestern Hokkaido, Japan. *Resource Geology,* 60(1), 52-70.

Jakni, B., Poupeau, G., Sosson, M., Rossi, P., Ferrandini, J., & Guennoc, P. (2000), Dénudations cénozoiques en Corse: une analyse thermochronologique par traces de fission sur apatites. *Comptes Rendus de Académié de Sciences Paris,* 331, 775-782.

Jolivet, L., Dubois, R., Fournier, M., Goffé, B., Michard, A., & Jourdan, C., (1990), Ductile extension in alpine Corsica. *Geology,* 18, 1007–1010.

Jolivet, L., Daniel, J. M., & Fournier, M. (1991), Geometry and Kinematics of ductile extension in Alpine Corsica. *Earth and Planetary Science Letters,* 104, 278- 291.

Jolivet, L., Faccenna, C., Goffé, B., Mattei, M., Rossetti, F., Brunet, C., Storti, F., Funiciello, R., Cadet, J. -P., D'Agostino, N., & Parra, T. (1998), Midcrustal shear zones in post-orogenic extension: Example from the Tyrrhenian Sea. *Journal of Geophysical Research,* 103, 12-123.

Jourdan, F., & Renne, P.R. (2007,. Age calibration of the Fish Canyon sanidine 40Ar/39Ar dating standard using primary K-Ar standards. *Geochimica Cosmochimica Acta,* 71, 387–402.

Koppers, A. A. P. (2002). ArArCALC-software for $^{40}Ar/^{39}Ar$ age calculations. *Computers and Geosciences,* 28(5), 605-619.

Lacombe, O., & Jolivet, L. (2005), Structural and kinematic relationships between Corsica and the Pyreneeses-Provence domain at the time of the Pyrenean orogeny. *Tectonics,* 24, TC1003. http://doi.org/10.1029/2004TC001673.

Lagabrielle, Y., & Polino, R. (1988), Un schéma structural du domaine des Schistes Lustrés ophiolitiféres au nord-ouest du massif du mont Viso (Alpes sudoccidentales) et ses implications. *Comptes Rendus de Académié de Sciences Paris,* 323, 957–964.

Lahondère, D., & Guerrot, C. (1997), Datation Sm-Nd du métamorphisme éclogitique en Corse alpine: un argument pour l'existence au Crétacé supérieur d'une zone de subduction active localisée sous le bloc corso-sarde. *Géologie de France,* 3, 3-11.

Lanari, P. (2012), Micro-cartgraphie P-T- dans les roches metamorphiques. Applications aux Alpes et à l'Himalaya, (doctoral dissertation). Université de Grenoble.

Laporte, D., Fernandez, A., & Orsini, J. B. (1991), Le complexe d'île Rousse, Balagne, Corse du Nord-Ouest: pétrologie et cadre de mise en place des granitoïdes magnésiopotassiques. *Géologie de France,* 4, 15-30.

Lardeaux, J. M., & Spalla, M. I. (1991), From granulites to eclogites in the Sesia Zone (Italian Western Alps)—A record of the opening and closure of the Piedmont ocean. *Journal of Metamorphic Geology,* 9(1), 35–59.

Law, R. D. (2014), Deformation thermometry based on quartz crystal fabrics and recrystallization microstructures: A review. *Journal of Structural Geology,* 66, 129–161.

Lee, J. -Y., Marti, K., Severinghaus, J. P., Kawamura, K., Yoo, H. -S., Lee, J. B., & Kim, J. S. (2006), A redetermination of the isotopic abundances of atmospheric Ar. *Geochimica et Cosmochimica Acta,* 70, 4507–4512.

Levi, N., Malasoma, A., Marroni, M., Pandolfi, L., & Paperini, M. (2007), Tectono- metamorphic history of the ophiolitic Lento unit (northern Corsica): evidences for the complexity of accrection-exhumation processes in a fossil subduction system. *Geodinamica Acta,* 20(1), 99-118.

Maggi, M., Rossetti, F., Corfu, F., Theye, T., Andersen, T. B., & Faccenna, C. (2012), Clinopyroxene-rutile phyllonites from East Tenda Shear Zone (Alpine Corsica, France): pressure-temperature-time constraints to the Alpine reworking of Variscan Corsica. *Journal of the Geological Society of London,* 169, 723–732.

Malasoma, A., & Marroni, M. (2007), HP/LT metamorphism in the Volparone Breccia (Northern Corsica, France): evidence for involvement of the Europe/Corsica continental margin in the Alpine subduction zone. *Journal of Metamorphic Geology,* 25, 529-545.

Malasoma, A., Marroni, M., Musumeci, G., & Pandolfi, L. (2006), High pressure mineral assemblage in granitic rocks from continental units, Alpine Corsica, France. *Geological Journal,* 41, 49-59.

Malasoma, A., Morelli, G., Di Rosa, M., Marroni, M., Pandeli, E., Principi, G.,

& Pandolfi, L. (2020), The stratigraphic and structural setting of metamorphic continental units from Alpine Corsica: clues from the area between Asco and Golo valleys (Central Corsica, France). *Journal of Maps,* 16(2), 313-323.

Malavieille, J., Chemenda, A., & Larroque, C. (1998), Evolutionary model for the Alpine Corsica: mechanism for ophiolite emplacement and exhumation of high-pressure rocks. *Terra Nova,* 10, 317–322.

Maluski, H., Mattauer, M., & Matte, P. H. (1973), Sur la presence de decrochement alpins en Corse. *Comptes Rendus de Académié de Sciences Paris,* 276, 709-712.

Maluski, H. (1977), Application de la méthode 40Ar/39Ar aux minéraux des roches cristallines perturbées par des événements thermiques et tectoniques en Corse. Ph.D, (doctoral dissertation). Université de Montpellier.

Manatschal, G. (1995), Jurassic rifting and formation of a passive continental margin (Platta and Err nappes, Eastern Switzerland): geometry, kinematics and geochemistry of fault rocks and comparison with Galicia margin, (doctoral dissertation). Zurich Universitat.

Marroni, M. (1991), Deformation history of the Mt. Gottero Unit (Internal Ligurid units, Northern Apennines*). Bollettino della Società Geologica Italiana,* 110(3-4), 727-736.

Marroni, M., & Pandolfi, L. (2003), Deformation history of the ophiolite sequence from the Balagne Nappe, northern Corsica: insights in the tectonic evolution of the Alpine Corsica. *Geological Journal,* 38, 67–83.

Marroni, M., & Pandolfi, L. (2007), The architecture of an incipient oceanic basin: a tentative reconstruction of the Jurassic Liguria-Piemonte basin along the Northern Apennine-Alpine Corsica transect. *International Journal of Earth Sciences,* 1059–1078.

Marroni, M., Meneghini, F., & Pandolfi, L. (2017), A revised Subduction Inception Model to Explain the Late Cretaceous, Double Vergent Orogen in the Precollisional Western Tethys: Evidence From the Northern Apennines. *Tectonics,* 36, 2227-2249.

Martin, A. J., Rubatto, D., Vitale Brovarone, A., & Hermann, J. (2011), Late Eocene lawsonite-eclogite facies metasomatism of a granulite sliver associated to ophiolites in Alpine Corsica. *Lithos,* 125, 620-640.

Massonne, H. J., & Schreyer, W. (1987), Phengite geobarometry based on the limiting assemblage with K-feldspar, phlogopite, and quartz. *Contributions to Mineralogy and Petrology,* 96, 212–224.

Mattauer, M., & Proust, F. (1976), La Corse alpine: un modèle de genès du metamorphisme haute pression par subdutcion de croute continentale sous du matériel océanique. *Comptes Rendus de Académié de Sciences Paris,* 282, 1249-1251.

Mattauer, M., Faure, M., & Malavieille, J. (1981), Transverse lineation and large- scale structures related to Alpine obduction in Corsica. *Journal of Structural Geology,* 3(4), 401-409.

Meneghini, F., Pandolfi, L., & Marroni, M. (2020), Recycling of heterogeneous material in the subduction factory: evidence from the sedimentary mélange of the Internal Ligurian Units, Italy. *Journal of the Geological Society,* 177, 587-599.

Ménot, R. P., & Orsini, J. B. (1990), Evolution du socle anté-stéphanien de Corse: événements magmatiques et métamorphiques. *Schweizerische Mineraogische und Petrographische Mittelungen,* 70, 35–53.

Meresse, F., Lagabrielle, Y., Malavieille, J., & Ildefonse, B. (2012), A fossil ocean- continent transition of the Mesozoic Tethys preserved in the Schistes Lustrés nappe of northern Corsica. *Tectonophysics,* 579, 4-16.

Michard, A., & Martinotti, G. (2002), The Eocene unconformity of the Brianconnais domain in the French-Italian Alps, revisited (Marguareis massif, Cuneo); a hint for a Late Cretaceous-Middle Eocene frontal bulge setting. *Geodinamica Acta,* 15, 289-301.

Molli, G., & Malavieille, J. (2011), Orogenic processes and the Corsica/Apennines geodynamic evolution: insights from Taiwan. *International Journal of Earth Sciences,* 100(5), 1207-1224.

Molli, G., & Tribuzio, R. (2004), Shear zones and metamorphic signature of subducted continental crust as tracers of the evolution of the Corsica/Northern Apennine orogenic system. In G. I. Alsop, R.E. Holdsworth, , K.J.W. McCaffrey, M. Handy (Eds.), *Flow Processes in Faults and Shear Zones, Geological Society of London Special Publications,* 224, 321–335.

Molli, G., Tribuzio, R., & Marquer, D. (2006), Deformation and metamorphism at the eastern border of Tenda Massif (NE Corsica): a record of subduction and exhumation of continental crust. *Journal of Structural Geology,* 28, 1748–1766.

Molli, G. (2008), Northern Apennine-Corsica orogenic system: an updated overview. In S. Siegesmund, B. Fugenschuh, N. Froitzheim (Eds.), *Tectonic Aspects of the Alpine-Dinaride-Carpathian System, Geological Society of London Special Publication,* 298, 413–442.

Pandolfi, L., Marroni, M., & Malasoma, A. (2016), Stratigraphic and structural features of the Bas-Ostriconi Unit (Corsica): paleogeographic implications. *Comptes Rendus de Académié de Sciences Paris,* 348, 630-640.

Paquette, J. L., Ménot, R. P., Pin, C., & Orsini, J. B. (2003), *Episodic and short-lived granitic pulses in a post-collisional setting: evidence from precise U-Pb zircon dating through a crustal cross-section in Corsica. Chemical Geology,* 198, 1- 20.

Passchier, C. W., & Trouw, R. A. J. (2005), *Microtectonics.* (Vol. 16). Berlin, New York, Springer.

Ramsay, J.G. (1967), *Folding and Fracturing of Rocks.* McGraw-Hill, New York.

Ravna, E. J. K., Andersen, T. B., Jolivet, L., & De Capitani, C. (2010), Cold subduction and the formation of lawsonite-eclogite from prograde evolution of eclogitized pillow lava from Corsica. *Journal of Metamorphic Geology,* 28, 381-395.

Rossetti, F., Glodny, J., Theye, T., & Maggi, M. (2015), Pressure temperature deformation- time of the ductile Alpine shearing in Corsica from orogenic construction to collapse. *Lithos,* 218-219, 99–116.

Rossi, P., Durand-Delga, M., Caron, J. M., Guieu, G., Conchon, O., Libourel, G., & Loye-Pilot, M. (1994), Carte Geologique de la France, feuille Corte (1110). *BRGM,* Orléans, scale 1:50000, 1 sheet.

Rossi, P., Oggiano, G., & Cocherie, A. (2009), A restored section of the "southern Variscan realm" the Corsica–Sardinia microcontinent. *Comptes Rendus Geosciences,* 341, 224-238.

Saccani, E., Padoa, E., & Tassinari, R. (2000), Preliminary data on the Pineto gabbroic massif and Nebbio basalts: progress toward the geochemical characterization of alpine Corsica ophiolites. *Ofioliti,* 25, 75-86.

Schmid, S. M., Pfiffner, O. A., Froitzheim, N., Schönborn, G., & Kissling, E. (1996), Geophysical–geological transect and tectonic evolution of the Swiss–Italian Alps. *Tectonics,* 15(5), 1036–1064.

Spear, F.S. (1993), The metamorphism of mafic rocks. In *Metamorphic phase Equilibria and Pressure-Temperature-Time paths*, *Mineralogical Society of America.*

Steiger, R. H., & Jäger, E. (1977), Subcommission on geochronology: Convention on the use of decay constants in geo- and cosmochronology. *Earth and Planetary Science Letters,* 36, 359–362.

Stipp, M., Stunitz, H., Heilbronner, R., & Schmid, S. M. (2002), Dynamic recrystallization of quartz: correlation between natural and experimental conditions. *Geological Society London special publications,* 200, 171-190. http://doi.org/10.1144/GSL.SP.2001.200.01.11

Tribuzio, R., & Giacomini, F. (2002), Blueschist facies metamorphism of peralkaline rhyolites from Tenda crystalline massif (northern Corsica): evidence for involvement in the Alpine subduction event? *Journal of Metamorphic Geology,* 20, 513-526.

Vidal, O., & Parra, T. (2000), *Exhumation paths of high-pressure metapelites obtained from local equilibria for chlorite–phengite assemblage. Geological Journal,* 35, 139–161.

Vitale Brovarone, A., & Herwartz, D. (2013), Timing of HP metamorphism in the Schistes Lustrés of Alpine Corsica: new Lu-Hf garnet and lawsonite ages. *Lithos,* 172-173, 175–191.

Vitale Brovarone, A., Beyssac, O., Malavieille, J., Molli, G., Beltrando, M., & Compagnoni, R. (2012), Stacking and metamorphism of continuous segments of subducted lithosphere in a high-pressure wedge: The example of Alpine Corsica (France). *Earth Science Reviews,* 116, 35-56.

Vitale Brovarone, A., Picatto, M., Beyssac, O., Lagabrielle, Y., & Castelli, D. (2014), The blueschist-eclogite transition in the Alpine chain: P-T paths and the role of slow-spreading extensional structures in the evolution of HP-LT mountain belts. *Tectonophysics,* 615, 96–121.

Warburton, J. (1986), The ophiolite-bearing Schistes Lustrés nappe in Alpine Corsica: a model for the implacement of ophiolites that have suffered HP/LT metamorphism. *Geological Society of America Bulletin Memoirs,* 164, 313-331.

Waters, C. N. (1990), The Cenozoic tectonic evolution of Alpine Corsica. *Journal of Geological Society of London,* 147, 811-824.

Zarki-Jakni, B., Van Der Beek, P., Poupeau, G., Sosson, M., Labrin, E., Rossi, P., & Ferrandini, J. (2004), Cenozoic denudation of Corsica in response to Ligurian and Tyrrhenian extension: results from apatite fission track thermochronology. *Tectonics,* 23, TC1003. http://doi.org/10.1029/ 2003TC001535